12-2005

Cloning, Overexpression, Purification and Characterization on N-Terminal Metal Binding Domains 5 and 6 of Wilsons Disease Protein

David Achila

CLONING, OVEREXPRESSION, PURIFICATION AND CHARACTERIZATION OF N-TERMINAL METAL BINDING DOMAINS 5 AND 6 OF WILSONS DISEASE PROTEIN

by

David Achila

A Thesis
Submitted to the
Faculty of The Graduate College
in partial fulfillment of the
requirements for the
Degree of Master of Science
Department of Chemistry

Western Michigan University
Kalamazoo, Michigan
December 2005

ACKNOWLEDGMENTS

I wish to sincerely thank Dr. David Huffman for granting me this research opportunity and for his insight, guidance and support during the project. I also wish acknowledge Dr. David Reinhold and Dr. Subra Murali for their guidance as the thesis committee members, Dr. Todd Barkman's lab group for sequencing the WD5-6 plasmid construct, Dr. Brian Tripp for use of spectrofluorimeter and the Department of Chemistry, Western Michigan University, for providing a conducive environment for this research project.

Secondly, I want to acknowledge the valuable contributions made by the Professor Ivano Bertini of CERM, Florence- Italy and his research group especially on the NMR experiments, Dr. Muralee Nair of Michigan State University for the use of spectropolarimeter, Ewa Folta-Stogniew of Yale Keck Facility for laser light scattering experiment and all others who aided in the completion of this work. Lastly, I wish to salute my family for their patience, endurance and encouragement throughout the time I was engaged in this work.

David Achila

CLONING, OVEREXPRESSION, PURIFICATION AND CHARACTERIZATION OF N-TERMINAL METAL BINDING DOMAINS 5 AND 6 OF WILSONS DISEASE PROTEIN

David Achila, M.S.

Western Michigan University, 2005

Wilsons disease is an autosomal recessive disorder of copper metabolism which results from mutations in the gene encoding for Wilson disease protein (WDP). The cytosolic N-terminus of WDP comprises six metal binding domains each containing a conserved metal binding motif, GMXCXXC. The contribution of these metal binding domains to copper homeostasis is poorly understood. We have cloned, expressed and purified residues 485 to 633 corresponding to N-terminal metal-binding domains 5 and 6 of WDP (WD5-6). Two of the 3 disease causing mutations in the N-terminal metal binding domains of WDP occur one in each of these domains and the two domains have been shown to be essential for copper induced response, catalytic phosphorylation and other functions of WDP.

We found that WD5-6 binds 2 equivalents of copper, has a pI of 4.97 and behaves as a monomer in solution. We also showed by NMR titration that WD5-6 accepts copper from the fourth metal binding domain of WDP, Cu(I)WD4, and not from Cu(I)Atox1, the copper chaperone that delivers copper to WDP. Solution NMR structure of apo-WD5-6 was elucidated and found to consist of 2 ferrodoxin-like folds that behaves as a unit in solution.

TABLE OF CONTENTS

Table of Contents – Continued

CHAPTER

Table of Contents – Continued

Table of Contents – Continued

CHAPTER

Table of Contents – Continued

LIST OF ABBREVIATIONS

CD..... Circular Dichroism

MNK..... Menkes Disease Protein

WD..... Wilsons Disease

WDP..... Wilsons Disease Protein

N-WDP..... N-terminal Metal Binding domains of WDP

XAS..... X-ray Absorption Spectroscopy

MBD..... Metal Binding Domain

DTT..... Dithiothreoerithritol

LIST OF TABLES

LIST OF FIGURES

List of Figures – Continued

CHAPTER I

INTRODUCTION

Copper homeostasis

Copper is an essential trace element that is a cofactor in several key enzymes (Linder, 1991). Some of the enzymes whose activity depend on copper are cytochrome c oxidase in the electron transport chain, superoxide dismutase for free radical detoxification, tyrosinase for melanin production, dopamine ß-hydroxylase for production of neurotransmitters and lysil oxidase for cross-linking collagen (Danks, 1980, 1995). Interaction of Cu with hydrogen peroxide rather than redox coupled partners can yield deleterious hydroxyl radical, which may lead to oxidative damage (DiGuiseppi & Fridovich, 1984). Therefore Cu is both essential as a redox catalyst in several oxidases and potentially deleterious due to its ability to cause DNA damage, inactivation of certain enzymes and lipid peroxidation when it accumulates in the tissues (Carmichael *et al.*, 1995; Gu *et al.*, 2000; Nair *et al.*, 1998).

Cu homeostasis must therefore be tightly controlled such that enough Cu is delivered to Cu-requiring enzymes while preventing excess build up in the cytoplasm. Proteins involved in the uptake, distribution, secretion and efflux of Cu include high affinity permeases for copper uptake, Cu chaperones for distribution to target Cu-requiring proteins, and Cu transporting P-type ATPases which transport Cu in the secretory pathway and export Cu when in excess (Huffman & O'Halloran, 2001; Prohaska & Gybina, 2004). The liver plays a crucial role in Cu balance in the body. Most

of the Cu absorbed from the intestine is received in the liver and biliary excretion of Cu is also closely connected to the liver (Tao & Gitlin, 2003).

Intracellular copper pathways

Cu is uptaken into the cell by a plasma membrane protein, Ctr1, which acts as a high affinity permease (Lee *et al.*, 2001). Cu(DiDonato *et al.*) is first reduced to Cu(Anastassopoulou et al.) during its uptake across the plasma membrane by mechanism that is still unknown (Lee *et al.*, 2002; Puig *et al.*, 2002). Extremely low free Cu ions exist in the cytoplasm (Rae *et al.*, 1999). Once in the cell, Cu is bound to Cu chaperones which deliver it to the target proteins through an efficient metallochaperone network (O'Halloran & Culotta, 2000) (Figure 1). In humans, Atox1 deliver Cu to the membrane associated Cu transporting ATPases; Wilson's disease protein (WDP) and Menkes disease protein (MNK), CCS delivers Cu to Cu/Zn superoxide dismutase (SOD) while Cox17 supplies cytochrome c oxidase with Cu. Other putative Cu handling proteins include Murr1 (Tao *et al.*, 2003), metallothionine (MT-1 and MT-2) and amyloid precursor protein (APP) (V. C. Culotta *et al.*, 1999; Prohaska & Gybina, 2004). WDP and MNK then use energy derived from ATP hydrolysis to translocate Cu into the secretory pathway and to export the excess into the bile (Hung *et al.*, 1997).

SOD is responsible for free radical detoxification. It catalyses the dismutation reaction of the toxic superoxide radical to molecular oxygen and hydrogen peroxide as follows;

$$\mathrm{Cu[II]\text{-}SOD} + \mathrm{O_2^{\cdot -}} \rightleftharpoons Cu[I] - SOD + O_2$$

$$Cu(I)-SOD+O_2^- +2H^+ \rightleftharpoons Cu(II)-SOD+H_2O_2$$

SOD thus forms a crucial part of the cellular antioxidant defense mechanism (Lavelle *et al.*, 1973; Paschen & Weser, 1973). Cytochrome c oxidase is a membrane protein which catalyzes reduction of the dioxygen molecule to water in the last step of electron transfer chain in cell as shown below.

$$4Fe^{2+}+4H^+ +O_2 \rightleftharpoons 4Fe^{3+}+2H_2O$$ (Tsukihara *et al.*, 1995)

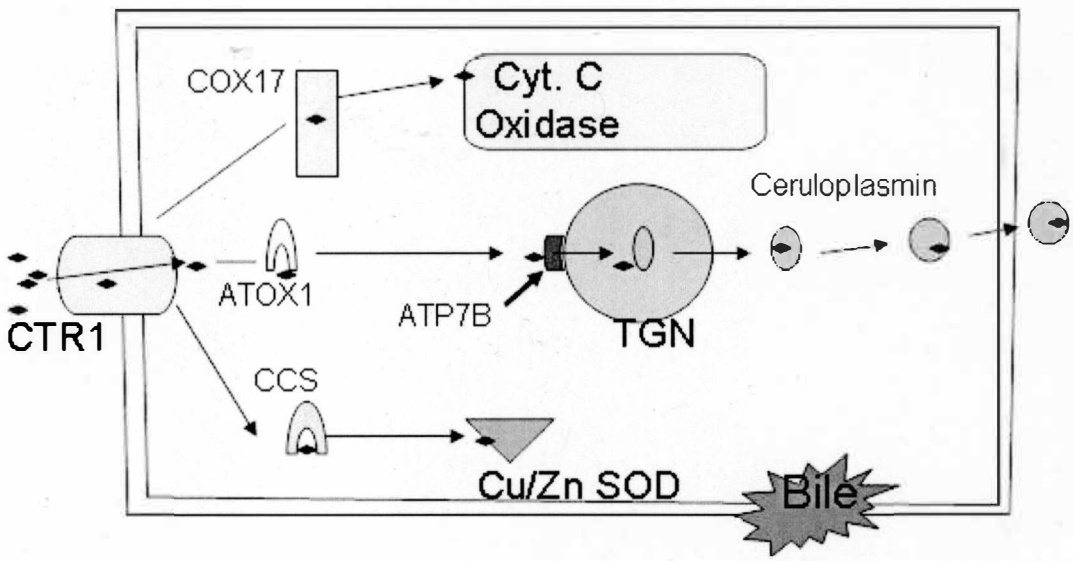

Figure 1. Intracellular pathways of Cu. Ctr1 permease imports Cu into the cell after which it is bound to various Cu chaperones; Atox1, CCS and Cox17. These metallochaperones in turn deliver Cu to target membrane proteins ATP7B (WDP) at TGN (trans-Golgi network) for translocation into different cell compartments, Cu/Zn SOD and Cyt c oxidase.

Wilson's disease

Wilson's disease is an autosomal recessive disorder of Cu metabolism. Patients accumulate Cu in the liver, kidney and to some extent, brain (Wilson, 1912). Wilson's disease affects 1/30,000 births worldwide (Gollan & Gollan, 1998). Common symptoms observed in patients include liver cirrhosis, degeneration of nervous system and renal dysfunction (Brewer & Yuzbasiyan-Gurkan, 1992). Most Wilson's disease patients have reduced Cu incorporation into ceruloplasmin, which is a multicopper oxidase in serum, (Scheinberg & Gitlin, 1952) and impaired biliary excretion (Frommer, 1974; Sternlieb, 1984).

Treatments that are used to manage Wilson's disease include chelating agents such as penicillamine and high doses of zinc salts (Gollan & Gollan, 1998). High doses of zinc salt prevent absorption of Cu. Cu may also play a role in Alzheimer's disease (Huang *et al.*, 1999) and prion diseases (Viles *et al.*, 1999)

Menkes disease

The importance of Cu homeostasis is underscored by Menkes and Wilson's disease (V. C. Culotta, Gitlin, JD, 2001; Danks, 1995), two related inherited diseases which show both the essential and toxic nature of Cu. Menkes disease is characterized by Cu deficiency due to defective transport across the placenta and intestinal uptake of Cu (Schaefer & Gitlin, 1999). Cu transport across the blood-brain barrier is also impaired leading to severe Cu deficiency in the central nervous system (Danks, 1995). Menkes

disease is caused by mutations in the gene coding for Menkes disease protein, MNK. The main symptoms of Menkes disease are neurological defects and eventual death in childhood (Schaefer & Gitlin, 1999). Prevalence rate reported for Menkes disease is 1:100,000 births (Danks, 1980). Intravenous administration of copper–histidine complex is the preferred treatment to Menkes disease (Christodoulou *et al.*, 1998).

Wilson's disease protein (WDP) and Menkes disease protein (MNK)

WDP and MNK are part of a large family of P-type ATPases found in most of life forms. They translocate Cu ions across vesicle membranes. WDP is localized in the trans-Golgi network (TGN) of hepatocytes where it transports Cu to key metalloenzymes such as ceruloplasmin in the secretory pathway (Hung et al., 1997). Analysis of cDNA of the two proteins reveals that they share 57% sequence homology (Cox, 1999). In bacteria, *E. hirae,* two ATPases CopA and CopB serve in uptake and efflux of Cu respectively. CopA shows extensive sequence identity to the MNK. Mutagenesis of CopB leads to Cu sensitive cells while disruption of CopA makes the cells Cu-dependent (Odermatt *et al.*, 1993). Ccc2 is the WDP homologue in yeast and it performs a similar function in yeast (Yuan *et al.*, 1995).

Structures of WDP and MNK

Both WDP and MNK have eight putative transmembrane domains of which the sixth bears a CPC (cystein-proline-cystein) motif which is thought to bind metal ions (Lutsenko *et al.*, 2002). In addition, there are six soluble N-terminal metal binding

domains each containing a conserved CXXC metal binding motif (Solioz & Vulpe, 1996)(Figure 2). The gene that encodes WDP is localized on chromosome 13 at loci q14.3. (Frydman *et al.*, 1985) WDP is 1411 amino acid residues long and is predicted to have a MW of 159 kD (Bull & Cox, 1994).

The yeast homologue of WDP, Ccc2, contains two N-terminal metal binding domains each bearing the conserved CXXC metal binding motif (Yuan et al., 1995). Human copper chaperone, Atox1, and its homologues found in both eukaryotes and prokaryotes contain a single CXXC motif (Elam *et al.*, 2002). The gene that encodes MNK is localized to q13 loci of the X-chromosome (Tonnesen *et al.*, 1992). MNK is expressed in all tissues other than the liver and is composed of 1500 amino acid residues (Vulpe *et al.*, 1993).

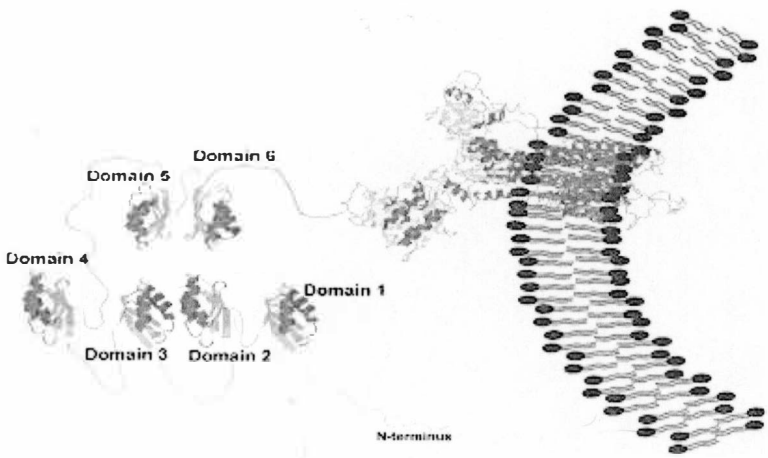

Figure 2. WDP model showing the six N-terminal metal binding domains and transmembrane domain by Huffman D.L.

Functions of WDP and MNK

WDP and MNK proteins function to transport Cu to enzymes synthesized within secretory compartments and to export excess Cu into the bile. These dual functions contribute to copper homeostasis. In order to carry out these functions, WDP and MNK are themselves regulated by several factors like Atox1 and Cu concentration.

Regulation of WDP and MNK

Even though Cu uptake through Ctr1 is a critical step in the supply of Cu to the liver cells, the continuous accumulation of Cu in hepatocytes of WD patients despite massive increases in the total hepatic Cu content suggest that Cu homeostasis is not regulated at the uptake step (Gitlin, 2003). Atox1 mediated Cu transfer activates WDP (Walker *et al.*, 2002). It has been shown that Atox1 can carry Cu to N- terminal WDP (N-WDP) as well as remove Cu from it. This points to the fact that both metallated and apo forms of Atox1 may contribute to the regulation of WDP activity (Walker et al., 2002).

Cu binding to N-WDP has been shown to induce a metal-specific conformational change in this protein (DiDonato *et al.*, 2000). This conformational change is tied to cytosolic Cu concentration so it's likely for Cu bound state of WDP to regulate the activity of the transporter (Fatemi & Sarkar, 2002). Circular dichroism (CD) spectroscopy data showed that Cu binding actually induces conformational changes in WDP (DiDonato et al., 2000). The Cu occupancy of WDP affects its intracellular localization, post-translational modification and activity (Vanderwerf *et al.*, 2001). Atox1 may play key role in these events by controlling the amount of Cu bound to the transporter and hence contribute substantially to the regulation of the intracellular

localization or post-translational modification of WDP while keeping it active at a wide range of Cu concentrations.

CD and X-ray absorption spectroscopy (XAS) have been used to characterize Zn binding to the N-WDP. It has been revealed that Zn is able to bind to this domain with stochiometry of 6:1 (Gross *et al.*, 2000). Zn binding induces a conformational change in the N-WDP too but the changes are completely different from those observed with Cu binding and leads to overall loss of secondary structure in the domain. XAS spectra show that Zn is ligated by nitrogen atoms and therefore has low affinity for the heavy metal-associated binding motifs where Cu binds. This difference in binding may serve as the basis for the metal-ion mediated regulation of the ATPase *in vivo* (Gross et al., 2000).

A study using the N-terminal model of WDP homologue in rat, rCBD, showed that rCBD undergoes metal-induced secondary and tertiary structural changes similar to those observed for WDP (Tsay *et al.*, 2004). Analysis of far UV CD spectra of rCBD suggests that Cu(I) binding to sensor N-MBD induces a conformational change (Tsay et al., 2004). Incubation of the metallated Atox1 with full length N-terminal metal binding domains of WDP lead to transfer of 6 Cu atoms per protein molecule. Incubation of Cu-Atox1 with full length WDP resulted in stimulation of WDP catalytic activity while incubation of Cu-WDP with apo-Atox1 lead to removal of Cu and down-regulation of the protein's catalytic activity (Walker et al., 2002).

Catalytic phosphorylation of WDP and MNK

In addition to its role as a cofactor to several enzymes, Cu has been shown to regulate crucial post-translational events such as protein phosphorylation. Cu modulates

phosphorylation of its key transporter in humans, WDP (Vanderwerf et al., 2001). Cu-induced phosphorylation was found to be fast and specific and it correlates with the intracellular location of WDP. Cu induced phosphorylation seemed to require the presence of the N-terminal domain of this protein. This discovery may be significant in understanding how Cu transport is regulated in mammalian cells (Vanderwerf et al., 2001). It was proposed that WDP phosphorylation could be among the molecular mechanisms by which Cu regulates its own metabolism cells (Vanderwerf et al., 2001).

MNK is transiently phosphorylated by ATP in a Cu-specific and dependent manner and appears to undergo conformation changes in accordance with the classical P-type ATPase model (Voskoboinik *et al.*, 2001). The data obtained from this study also suggest that the catalytic cycle of the MNK protein begins with the binding of Cu to the high affinity binding sites in the transmembrane channel, followed by ATP binding and transient phosphorylation.

Interaction between Atox1 and WDP

Human Cu chaperone, Atox1, plays a key role in Cu distribution to the secretory pathway of the cell. Some insight on the interaction between WDP and atox1 has been got from studies done on yeast. Atx1 which is the Atox1 ortholog in yeast has been shown to transfer Cu to Ccc2, which transports Cu into the late Golgi compartment (Pufahl *et al.*, 1997). This point is supported by evidence from an experiment involving a deletion of the Atox1 gene in mice leading to intracellular Cu accumulation and decreased activity of secreted Cu dependent enzymes such as tyrosinase (Hamza *et al.*, 2001).

Several studies have shown evidence for physical interaction between Atox1 and some of the N-terminal metal binding domains of WDP and MNK (Hamza *et al.*, 1999; Larin *et al.*, 1999; Lockhart & Mercer, 2000; van Dongen *et al.*, 2004). A study utilizing a glutathione S-transferase-Atox1 fusion protein showed direct protein-protein interaction between Atox1 and WD1-4 which is dependent on the presence of copper ligands, CXXC, in the N-terminus of Atox1 (Hamza et al., 1999). This finding was supported by a coimmunoprecipitation experiment which revealed that Atox1 interacts with both WDP and MNK in the cells in a Cu dependent manner (Hamza et al., 1999). A similar study carried out to test disease-associated mutations in the N-WDP showed a decrease in Atox1 interaction with mutated WDP proteins (Hamza et al., 1999). Impaired Cu delivery by Atox1 is thought to constitute a molecular basis of Wilson's disease in patients harboring these mutations (Hamza et al., 1999).

A systemic yeast two-hybrid screening of interaction between Cu binding domains showed that Atox1 interacts with MBDs 2 and 4 of WDP. Other interactions detected are between Atx1 with Ccc2, MBDs 2 and 4 of WDP. WDP MBD 4 showed the strongest interaction with Atox1 and Atx1 of all the 6 single metal binding domains (van Dongen et al., 2004). All the interactions between Atox1 and single copper binding domains were found to be weaker than interaction between Atox1 with the fragment containing the first four copper binding domains of WDP (van Dongen et al., 2004). Interaction between Atox1 and the first four copper binding domains had been shown to be strong (Larin et al., 1999). It had been shown earlier that Atox1 interacts with MBDs 1, 2 and 3 of WDP (Larin et al., 1999). No interaction was shown between any two single

copper binding domains of WDP and Ccc2. Metal binding domains 5 and 6 showed no interaction with Atox1 (van Dongen et al., 2004).

The transfer of one Cu metal ion from Atox1 to N-WDP results in selective shielding of cysteine in MBD2 against labeling with a cysteine-directed probe, a fact that is not observed when free Cu is added to MBD2 (Walker *et al.*, 2004). It was also realized that site-directed mutagenesis of MBD2 knocks out the stimulation of the catalytic activity of WDP by the Cu-Atox1 complex but not by free Cu. Based on these results, the authors suggested that Atox1 specifically delivers Cu to MBD2 of WDP (Walker et al., 2004). The authors also proposed that the preference of Atox1 for MBD2 may not be due to higher Cu binding affinity of MBD2 compared to the other five MBDs nor appropriate exposure of the metal coordinating residues but is likely due to specific protein-protein interactions. This specific interaction is enabled by the complementation of the negatively charged patch at the surface of MBD2 and positively charged patch on Atox1.

The authors observed that Cu bound to MBD2 didn't migrate to the other MBD and this fails to support the idea that MBD2 may be the entrance point of Cu transfered from Atox1 into N-WDP, but rather, suggests that Cu binding to MBD2 is likely to work as a switch allowing subsequent loading of other sites. MBD2 was found to retain Cu much better than Atox1 by competition experiments using a Cu chelator. This may promote metal transfer process from Atox1 to MBD2.

Electrostatic surface complementation between P-type ATPases and copper chaperones

The solution NMR structure of Ccc2a, the first MBD domain of WDP homologue in yeast, revealed a negatively charged patch near the Cu binding region (Banci *et al.*, 2001). The negative patch is formed by the presence of several glutamate and aspartate residues including two aspartates and one glutamate that are largely conserved among metal-transporting ATPases (Banci et al., 2001). A very similar negative patch is evident in generated structure of fourth MBD of human MNK (Gitschier *et al.*, 1998). A complimentary array of lysine and arginine residues in the vicinity of the metal binding site of Atx1 forms a positively charged patch (Rosenzweig *et al.*, 1999)(Figure 3). These complimentary surface charges may play a crucial part in the interaction and Cu exchange between Atx1 and the target MBD.

Copper coordination by WDP and Atox1

X-ray absorption spectroscopy (XAS) studies on MBD2 of WDP found that it coordinates Cu in a similar manner as Atox1. EXAFS experiments showed that MBD2 and Atox1 bind Cu^{+} with a linear coordination and the distance between sulfurs in the cysteine residues to the Cu is 2.16Å (Ralle *et al.*, 2003). This observation hints at the fact that the near non-coordinating ligands in the MBS2 and Atox1 are responsible for the difference in their Cu binding properties (Walker et al., 2004).

Electron paramagnetic resonance (EPR) analysis of Cu bound MBD1 of MNK showed no signal. This confirmed that Cu bound to MBD1 is in the +1 oxidation state and not +2 (Jensen *et al.*, 1999). Cu (I) binds to MBD1 of MNK in a 1:1 stochiometry with an apparent K_d of 46 μM., according to an equilibrium dialysis study carried out by

the Jensen's group. Oxidized MBD1 was, however, found not to bind Cu (Jensen et al., 1999). It was also found that N-WDP and N-MNK readily bind Cu both *in vitro* and *in vivo* with a stochiometry of 6.5-7.3 per N-WDP or N-MNK (DiDonato et al., 1997) leading to a suggestion that each of the six MBDs is involved in Cu coordination.

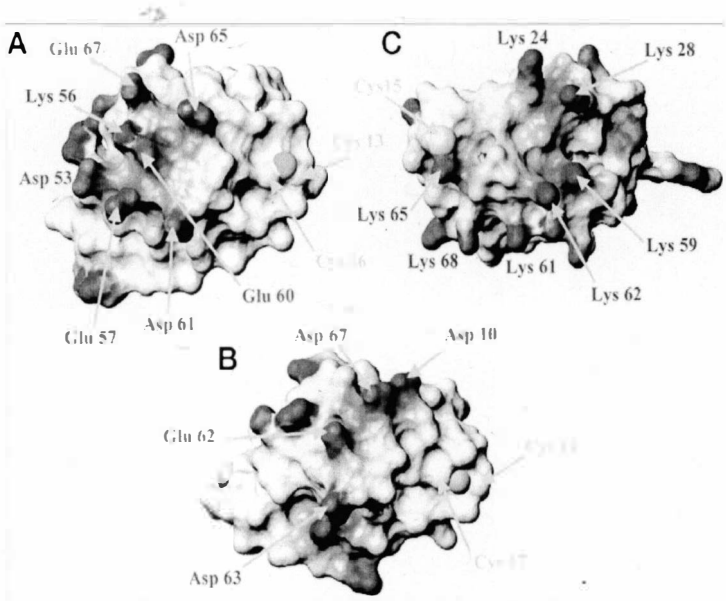

Figure 3. Electrostatic potential surface of the Cu(I)-Ccc2a, (A), Ag(I)-MBD4 (MNK), (B) and Cu(I)-Atx1, (C) (Banci et al., 2001).

Metal ion specificity

Several studies have shown that despite a high level of sequence similarity, P1-type ATPases are very discriminative in transporting metal ions. For example an E. coli P-type ATPase, ZntA, is specific for ions Pb(II), Zn(II), Cd(II), and Hg(II), while WDP, MNK and CopA (from *E.coli*) and homologues transport Cu(I) and possibly Ag(I). A study using a chimeric protein of ZntA with the N-terminal domain interchanged with either the whole N-WDP or only the sixth MBD of WDP replacing the N-terminal of

ZntA found that both chimeras conferred resistance to lead, zinc, and cadmium salts but not Cu salts. The purified chimeras displayed ATPase activity with zinc, lead, mercury and cadmium which are all ZntA substrates, but no activities for Cu or silver, which are WDP substrates. The chimeras were also less active than wild type ZntA.

The N-terminal domain cannot alter metal specificity dictated by the transmembrane segment and it interacts with the rest of the transporter in a metal ion-specific manner (Mitra & Sharma, 2001). A related study found that Zn actually binds WDP but is ligated to nitrogen atoms and not sulfur as for Cu. This binding also induces a conformational change different from the one observed upon Cu binding. This may suggest a possible structure-based mechanism for the discrimination of different metal ions *in vivo* (DiDonato *et al.*, 2002).

WDP and MNK were found to be discriminative in the metal ion that they bind and transport across the membrane. A study using immobilized metal ion chromatography revealed that the fusion protein of N-WDP is able to bind transition metals with different affinities as follows: Cu(II)>>Zn(II)>Ni(I)>Co(II). Zn (II) only binds in the pH range of 6.5 to 9.0. N-WDP however showed no affinity for Ca(II) and Mg(II) compared to Cu. It also did not bind Fe (II) and Fe (III) (DiDonato et al., 1997).

Copper-induced relocalization of WDP and MNK

Under normal copper concentration, WDP and MNK are localized in the trans-Golgi network(TGN) where they help incorporate Cu(I) ions into copper-dependent enzymes, but when copper levels are elevated, most of the MNK traffic from the TGN to

the plasma membrane, while WDP relocates primarily to the intracellular vesicular compartments (Pena *et al.*, 1999; Strausak *et al.*, 1999).

N-terminal metal binding domains of WDP and MNK

WDP and MNK each have six metal binding domains (MBD) which are about 70 amino acids long and share 20-60% homology at their N-terminus. This low similarity in sequence suggest that they may be functionally non-equivalent, possibly with respect to interaction with the copper chaperone Atox1 (Hamza et al., 2001; Hamza et al., 1999). The solution NMR structure of the fourth MBD of MNK shows that it has a compact structure with βαββαβ 'ferredoxin-like' fold (Gitschier et al., 1998). This structure, which was determined by heteronuclear NMR method, however, differs from the crystal structure of the same protein in which two Atox1 molecules coordinate a single metal ion with retention of the βαββαβ fold (Wernimont *et al.*, 2000). The solution NMR structure of apo- and Cu(I)-Ccc2a from yeast also showed a ferrodixin-like fold (Figure 4).

A Cu binding site, CXXC, is housed in the highly conserved motif GMTCXXC which forms a loop within each of the MBDs. Conserved residues in all MBDs are clustered close to this loop thereby forming a suitable environment necessary for accepting Cu from intracellular Cu donors such as Atox1. Cu-induced conformational analysis showed that both secondary and tertiary structural changes take place upon Cu binding. These changes are thought to play both regulatory and functional roles in vivo (DiDonato et al., 2000).

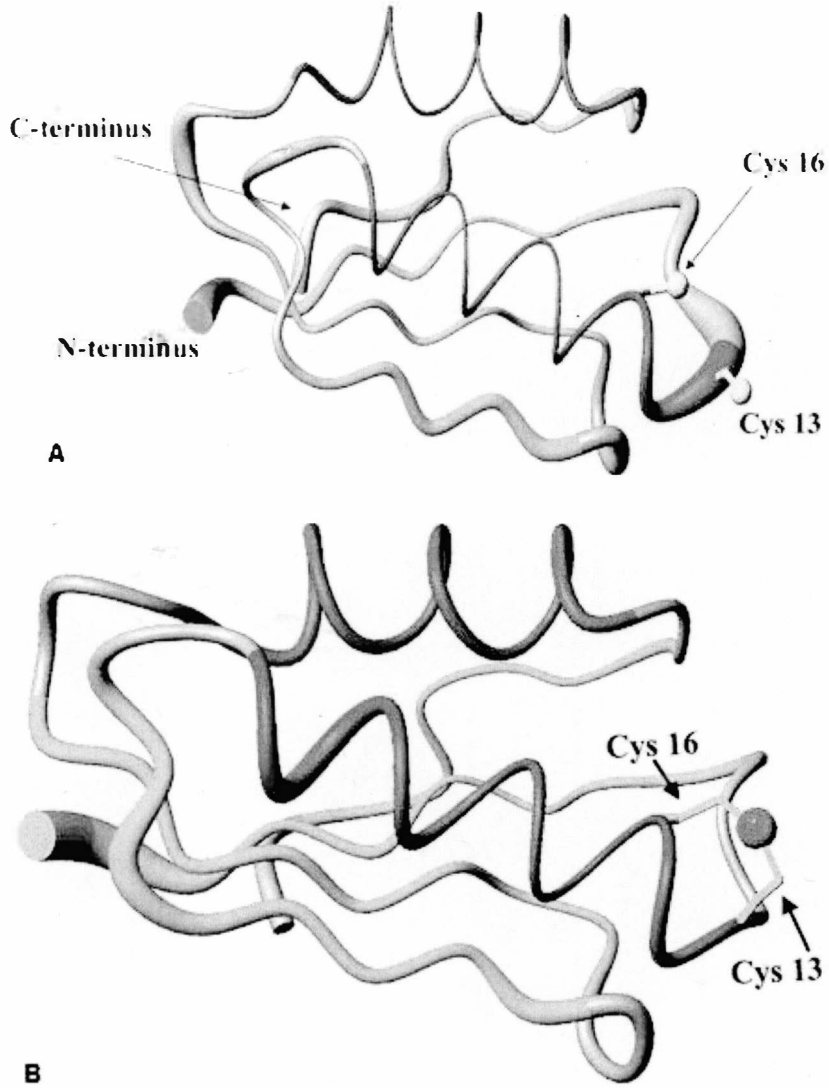

Figure 4. Backbone atoms for the solution structure of apo-Ccc2a (A) and Cu(I)-Ccc2a. (B) A tube with variable radius proportional to the backbone residue mean standard deviation value of each residue (Banci et al., 2001).

Non-equivalency of MBDs

The function of the six MBDs of WDP and MNK in Cu balance is not well understood. Several genetic and biochemical studies suggest that MBDs perform different functions. Yeast complementation assays indicate that MBD 6 alone is sufficient

for loading Cu into Fet3, the yeast homologue of cerulloplasmin. (Forbes *et al.*, 1999; Iida *et al.*, 1998). The second and third MBDs could not substitute for the sixth MBD in loading Cu to Fet3. Put together these findings suggest distinct functions for individual domains. Moreover a study done using WDP variants with mutations or truncation in the N-WDP found that Cu stimulates catalytic activity cooperatively and that this requires the presence of MBDs 5 and 6 (Huster & Lutsenko, 2003). Mutations in MBD6 or MBDs1-5 lead to non-cooperative activity of WDP by Cu whereas deletion of MBD1-4 doesn't affect cooperative catalytic phosphorylation activity of WDP (Huster & Lutsenko, 2003). MBDs 5 and 6 together regulate the affinity of intra-membrane binding sites for Cu.

These data imply that MBDs 5 and 6 may be more functionally important than MBDs 1-4, which are thought to control access of Cu to these later domains (Huster & Lutsenko, 2003). This findings are in contrast to those of yeast complementation studies on MNK which show that MBDs 1-4 are important for Cu transport (Payne & Gitlin, 1998). MBDs 4-6 of MNK were found to be essential for relocalization of MNK from the trans-Golgi network to the plasma membrane in response to Cu elevation in the cell (Voskoboinik *et al.*, 1999).

Association constant and stoichiometry of Cu (I) binding

A study using isothermal titration calorimetry (Frydman et al.) to measure the association constant K_a and stoichiometry (n) values for Cu(I) binding to WDP MBDs and Atox1 found that the association constants range from 10^5 M^{-1} to 10^6 M^{-1} and are similar for the chaperone and target domains (Wernimont *et al.*, 2004). These results therefore imply that Cu handling by Atox1 and Cu exchange between the chaperone and

WDP are under kinetic and not thermodynamic control. The same study also showed that Cu binding properties of each domain are affected by the presence of the other domains. The MBDs have similar affinities so their functional differences may be conferred by the protein fold and electrostatic surface properties.

Mutations in the WDP gene

More than 100 mutations have been found in the gene encoding WD (Krawczak & Cooper, 1997). Three well characterized disease causing mutations have been detected in N-WDP. These mutations have been identified as G85V in MBD1, L492S in MBD5 and G591D in MBD6 (Loudianos *et al.*, 1996). All three mutations are in the highly conserved regions. This implies an essential structural role of these MBDs. Molecular modeling of these missense mutations using the NMR solution structure of the fourth copper-binding domain of the MNK indicates the potential of these mutations to disrupt the tertiary structure of this region (Loudianos et al., 1996).

The mutant proteins were found to be express at the same level as the wild type protein in cells by immunoblot analysis (Hamza et al., 1999). The mutants were found to be localized at the trans-Golgi network, the same as in the wild type, by immunofluorescent microscopy. Each of the 3 mutations, however, led to decreased interaction with Atox1 (Hamza et al., 1999). Another mutant, P985A, showed no decrease in Atox1 binding under the same conditions. The discovery that WDP mutations disrupt Atox1 binding is significant and may be very helpful in the search for a cure for WD. These data imply that binding of Atox1 to N-WDP is important in Cu homeostasis

(Hamza et al., 1999). Atox1 is therefore a possible target for therapeutic approaches aimed at treating WD

WD5-6

These are the two N-WDP MBDs nearest to the membrane. They consist of 149 amino acid residues (Figure 5) with a predicted molecular weight of 16,049 Da. There are two metal binding motifs, CXXC, one in each of the domains. The unique short linker between these two domains is also present in orthologs bearing two or more MBDs in other species (Arnesano *et al.*, 2002). The longest linker of about 57 residues in WDP occurs between MBD 4 and MBD5 (Arnesano et al., 2002) which suggests that MBD5 and MBD6 may operate as a unit and therefore present an excellent module for studying the influence of one domain on another. Two of the three missense disease causing mutations in the N-WDP occur in MBD5 and MBD6 (Loudianos et al., 1996). These mutations have been shown to abrogate the interaction between N-WDP domains and the Cu chaperone, Atox1, with N-WDP (Hamza et al., 1999). Presence of MBDs 5 and 6 and not MBDs1-4 was shown to be essential for the cooperative catalytic phosphorylation activity of WDP (Huster & Lutsenko, 2003). These two domains have also been found to be essential for the Cu-induced trafficking of WDP from the trans-Golgi network region to the plasma membrane (Voskoboinik et al., 1999).

481 APQKC F QIKGMTCA SCVSNIERNL QKEAGVLSVL VALMAGKAEI KYDPEVIQPL

541 EIAQFIQDLG FEAAVMEDYA GSDGNIELTI TGMTCASCVH NIESKLTRTN GITYASVALA

601 TSKALVKFDP EIIGPRDIIK IIEEIGFHAS LAQ

Figure 5. Amino acid sequence for WD5-6 protein. Residues highlighted in green are the mutations in MBD5 (L492S) and in MBD6 (G591D). Cysteins that participate in copper coordination are highlighted in red and the residues highlighted in blue are the highly conserved methionine residues which are part of the metal binding motif.

Significance of this study

Wilson's disease affects Cu balance in the body leading to severe liver cirrhosis, neurodegenerative disorders and other serious symptoms (Wilson, 1912). The discovery of proteins that uptake, distribute, store and efflux excess Cu opened a new frontier in the search for a cure for this disease (O'Halloran & Culotta, 2000). Several treatments for WD have been developed but more specific information on the molecular parthenogenesis of this disease is still lacking. The N-terminal metal binding domains of WDP and MNK play an important role in receiving Cu from the chaperones (Forbes et al., 1999) and initiating catalytic activity through interaction with the chaperones (Vanderwerf et al., 2001).

Two of the three disease causing mutations in the N-WDP occur in WD5-6, one in each of the domains (Loudianos et al., 1996). These mutations are thought to disrupt interaction of the full length N-terminal metal binding domains with Atox1, which delivers Cu to WDP. Therefore full characterization of these two domains may greatly enhance our understanding of regulation of WDP functions and how disruption of its function affects Cu homeostasis.

Several structural studies of single metal binding domains of P-type ATPases have been reported. Solution NMR structure of Cu(I) bound and apo forms of the second (Banci *et al.*, 2004), the fourth (Gitschier et al., 1998) MBDs of the MNK, Cu(I) and apo forms of yeast copper transporter domain Ccc2a, (Banci et al., 2001) have also been elucidated. No solution NMR structure of any of the six metal binding domains of WDP has been reported yet. WD5-6 is a unique multi-domain construct because the two domains seem to be more functionally important and bear a short linker between them, preceded by a long linker between domains 4 and 5. This is the first structural study of a multi-domain construct of N-WDP domains reported to date.

It's been shown that WD5 and WD6 don't interact with Atox1 (van Dongen et al., 2004) and therefore may be receiving Cu from the other domains that interact with the Atox1. Two domains that have been shown to interact with Atox1 are MBD2 and MBD4 (van Dongen et al., 2004). MDB4 interaction with Atox1 is, however, much stronger than that of MBD2 (van Dongen et al., 2004). We are therefore interested in knowing how WD5-6 acquires Cu and how the 2 disease causing mutations in WD5-6 affect Cu this process. We propose here that WD5-6 has a ferrodoxine-like fold and that WD4 is a possible Cu donor for WD5-6.

Objectives of this study

In this study we focused on cloning, expression, purification and characterization of WD5-6 using various spectroscopic and chromatographic techniques. The other

objectives of this study were to elucidate of solution NMR structure of WD5-6 and to test interactions between WD5-6 with metallated WD4 and Atox1 by NMR titration.

CHAPTER II

EXPERIMENTAL METHODS

Materials

All the primers were purchased from Integrated DNA Technologies, Inc. All restriction endonucleases, other enzymes and their buffers were purchased from New England Biolabs Inc. and Life Technologies. The nucleotides and citric acid were purchased from Sigma Chemicals Co., while the bacterial strains and plasmids were obtained from Novagen. The QIAGEN plasmid DNA isolation kit was purchased from Qiagen Inc. Dimethylsulfoxide (DMSO) and dibasic potassium phosphate were purchased from J. T. Baker Chemical Co. Isopropyl-β-D-thiogalactopyranoside (IPTG) was purchased from INALCO SPA (Milano, Italy).

Sodium chloride, ammonium sulfate, 2-(4-Morpholino)-ethane sulphonic acid, dextrose, yeast extract, thiamine hydrochloride and sodium phosphate (mono- and dibasic) were purchased from Fisher Chemicals. Deuterium oxide (D_2O) was obtained from Aldrich, tris-(2-Carboxyethyl)-phosphine hydrochloride (TCEP.HCl) used as a reducing agent during fluorescence experiments was bought from Pierce, Bio-Rad dye for determination of protein concentration from Bio-Rad Laboratories Inc., Agarose from Gibco BRL, Kanamycin sulphate recombinant plasmid screening from Calbiochem and Bacto-Agar from DIFCO laboratories. PES (polyether sulfone) filter (0.22 μm) used to filter the extracted protein were purchased from Corning Inc. Stirred Ultra-filtration Cells obtained from Amicon Bioseparations while NMR tubes were bought from WILMAD LabGlass.

Cloning of WD5-6 gene

To produce WD5-6, the gene coding for WD5-6 protein was amplified by PCR from cDNA copy, digested by restriction enzymes then inserted into an appropriate expression vector. The recombinant plasmid is transformed and induced in *E. coli* cells for protein expression.

Primer design

Forward primer, 5'-CAA CCA GAG CCA TGG CAC CGC AGA AG-3', was designed to include a start codon ATG (Met) and a unique restriction site for Nco1 (CCATGG) while the reverse primer, 5'-GAG CGT TGG GAT CCT ACT GGG CCA GGG-3', was designed to include a stop codon (ACT) and a unique restriction site for BamH1 (GGATCC). The primers were used to amplify the gene coding for WD5-6 from human cDNA for full length wild type template of Wilson's disease protein using polymerase chain reaction (PCR) thermal cycling.

Amplification of WD5-6 gene by PCR

The gene encoding WD5-6 was amplified by PCR thermal cycling using the following program: (1) initial melting of the template DNA at 95 ˚C for 5 min so that it is denatured into two strands, (2) annealing step at 65 ˚C for 1 min so that primers can hybridize to the template DNA strand, (3) extension of primers by the DNA polymerase at 72 ˚C for 40 sec (4) denaturing at 95 ˚C for 40 sec, (5) annealing at 65 ˚C for 1 min (6) extension at 72 ˚C for 1 min. Steps 4-6 were repeated 28 times then stored at 4 ˚C for 24

hours. Annealing temperature (T_m) was calculated from the composition of the primers according to Wallace rule (equation 2.1)

$$T_m \text{ (in } ^0C) = [(G+C) \times 4 + (A+T) \times 2] \qquad 2.1$$

PCR product was then purified by QIAquick Spin PCR Purification Kit (Qiagen, Inc.) in three principle steps which includes; binding of the DNA to a column, washing and finally eluting in an elution buffer by use of microcentrifugation according to the kit instructions from the manufacturer. The size of purified DNA was determined by running the purified PCR product on a 2% agarose gel alongside 100 base pairs DNA marker for 1 hour at 70 volts. The gel was stained with ethidium bromide for 20 min then visualized under UV light. The size and concentration of the desired protein was determined by comparing it to the standard DNA markers according to manufacturer's instructions.

Construction of an expression vector for WD5-6

An expression vector for WD5-6 gene was prepared by ligating WD5-6 insert digested by NcoI and BamHI restriction enzymes to similarly digested pET24d+ to form a recombinant expression vector, pDAWD5-6. The ligation was achieved by use of ligase enzyme at 16°C for 8 hours. Heat-bar in a 4°C cooler was used to maintain a constant temperature. The ligation products were analyzed by 1% agarose gel electrophoresis.

Amplification and analysis of the recombinant plasmid

To amplify the WD5-6 recombinant plasmid, the plasmid was transformed into *E. coli* cells, grown in LB media then isolated as described below.

Transformation of pDAWD5-6 into DHα5 cells

The recombinant plasmid was maintained in *E. coli* DH5α host cells. Two aliquots of DH5α cells were thawed on ice before addition of 3 μL of dimethylsulfoxide (DMSO). Undigested pET24d+ was added to the positive control tube, 2 ng of double-digested pET24d+ was added to the first negative control tube, 2 ng of recombinant plasmid to the experimental tube and nothing was added to the second negative control tube. The cells were incubated on ice for an additional 30 min then subjected to heat shock at 42°C for 1 min. After heat shock, they were incubated on ice for 1 min then resuspended in 1 mL LB media containing no antibiotic. They were then incubated at 37°C and rotated at 250 rpm shaker for 1 hour. Finally the cells were centrifuged at 14,000 rpm for 1 min using a microcetrifuge, resuspended in 0.2 mL of LB and plated out on LB plates containing 30 μg/mL of kanamycin. After 20 min, the plates were put in a 37°C incubator for 12 hours.

Inoculation of transformed cells

A single colony from the experimental plate was aseptically picked and introduced into 5 mL of LB culture containing 30 μg/mL of kanamycin. The culture was then incubated at 37 ^{0}C and rotated at 250 rpm until the optical density at 600 nm (OD_{600})

reached 1. The cells were pelleted at 14,000 rpm for 2 min using a microcetrifuge. Plasmid DNA was recovered and purified using a plasmid recovery kit from Qiagen Inc.

Analysis of recovered plasmid

The purified recovered recombinant plasmid was first ran on a 1% agarose gel to ascertain the size, then subjected to restriction analysis and sequencing to confirm if the insertion was successful. Restriction analysis was done by digesting the recombinant plasmid with BamH1 and BglII restriction enzymes for 12 hours at 37 ^{0}C then the fragments were run on a 1.5 % agarose gel to determine the size of the excised piece. Gene sequencing was done in Dr. Barkman's laboratory to that the correct sequence was obtained.

Induction of WD5-6

Having confirmed the insertion of the WD5-6 gene into the expression vector, an induction test was set up to evaluate whether the recombinant plasmid could be induced to produce the protein of interest in *E. coli* cells. The plasmid was transformed in BL21 (DE3) cells by the same procedure used above then plated on LB agar plates containing 30 µg/mL kanamycin sulfates. Undigested pET24d+ vector was used as the positive control while double digested pET24d+ was used as negative control. A single colony from the experimental plate was inoculated into 5 mL of LB medium containing 30 µg/ml kanamycin sulfate then incubated in a shaker set at 37°C and rotated at 250 rpm untill an OD_{600} of approximately 0.6 was reached.

The culture was pelleted by centrifugation then resuspended in 100 mL of LB medium containing 30 μg/mL of kanamycin. The culture was incubated as described before. At OD_{600} = 0.45, protein production was induced by addition of 1 mM isopropyl-beta-thiogalactopyranoside (IPTG). The change in OD_{600} was monitored every 30 min and each time a 0.5 mL sample was withdrawn, centrifuged and later loaded onto a 15% tricine sodium dodecyl sulfate-polyacrylamide gel (SDS-PAGE) in a Hoefer SE 250 mini-vertical gel electrophoresis unit. The pellets were first treated with 5 μL of loading buffer and 20 μl of water then heated at 92 ^{0}C for 5 minutes before loading onto the gel. The gel was run at 72 V for 1 hour then stained with coomassie blue strain for four hours. The gel was destained, and then dried using a mini gel drying system from Invitrogen.

Overexpression of WD5-6

Having shown that induction of the WD5-6 protein in DE3 cells was efficient, it was then overexpressed in 10 L of LB medium. A fresh colony of BL21 (DE3) cells transformed with pDAWD5-6 recombinant plasmid was inoculated in 5 mL LB media containing 30 μg/ml of kanamycin and grown in a 37°C incubator to an OD_{600} of about 1. The culture was pelleted, then resuspended in 100 mL LB containing the same concentration of kanamycin and grown to the same OD_{600}. This was used as a starter culture to inoculate 10 L LB. This big batch culture of BL21 (DE3) transformed with pDAWD5-6 was grown aerobically in a Microferm Fermentor (New Brunswick Scientific Co.) to an OD_{600} of 0.45 before WD5-6 expression was induced with 1 mM

IPTG. After 3 hr the cells were harvested by centrifugation at 6000 RPM for 15 min using a SLA 3000 rotor. The cell pellets was stored at -20 °C prior to protein extraction.

WD5-6 extraction and purification

WD5-6 extraction

Protein extraction was done by treating the cell pellets with three successive cycles of 10 min freezing in liquid nitrogen and 15 min thawing at 25°C. The pellet was resuspended in 240 mL of freeze-thaw extraction buffer (20mM MES/Na, pH6, 0.1 mM EDTA, 1mM dithiothreitol (DTT)) then incubated on ice for 1 hr with periodic gentle agitation followed by centrifugation at 6000 rpm for 15 min using a SLA-3000 rotor at 4°C. The supernatant was vacuum filtered through a 0.22 μm filter then stored at -20 °C. The WD5-6 protein was purified in two chromatographic steps; Ion exchange and gel filtration chromatography.

Ion exchange chromatography (IEC)

The WD5-6 extract was thawed on ice then loaded onto a pre-equilibrated DEAE-Sepharose column (Pharmacia, 2.6 cm X 13 cm, 69 mL). The protein was eluted with a linear NaCl gradient using two buffers; (a) 20mM MES/Na, pH6, 0.1 mM EDTA, 5mM DTT and (b) 20mM MES/Na, pH6, 0.1 mM EDTA, 1 M NaCl, 5mM DTT. Every 3rd elution fraction was tested for protein content by Bio-rad protein assay. The WD5-6 protein containing fractions were identified by SDS-PAGE. All the WD5-6 containing

fractions were pooled and concentrated using an Amicon device fitted with an YM-3 membrane.

Size exclusion chromatography (SEC)

The concentrated protein solution was loaded onto a superdex-G75 26/60 Hi-Load column (Amersham Biotech) attached to fast protein liquid chromatography (FPLC) and eluted with a 20 mM MES/Na, pH 6.0, 150 mM NaCl, 10 mM DTT buffer. DTT was included to ensure WD5-6 is reduced and running as a monomer. The elution was monitored by UV spectrophotometry. Biorad protein assay was used to test for protein containing fractions while SDS-PAGE was used to evaluate the purity of the WD5-6. The fractions containing WD5-6 were pooled together and concentrated by an Amicon device. Concentrated WD5-6 protein solution was stored in 0.2 mL aliquots at -80°C.

Isotopic labeling of WD5-6

Solving solution NMR structures of large proteins requires higher dimensional NMR experiments (2D and 3D) that can only be achieved by isotopically labeled proteins. Isotopic labeling was done to produce proteins uniformly labeled with ^{13}C and/or ^{15}N for solution structure determination by NMR. The same expression vector and host cells used for the unlabeled protein were employed but this time cells were grown in minimal media. An induction test similar to the one described above was done in minimal media supplemented with unlabeled dextrose and ammonium chloride as the sole glucose and nitrogen source respectively. ^{15}N Labeled WD5-6 was produced by growing BL21

(DE3) cells transformed with pDAWD5-6 in 2 L of minimal media supplemented with [^{15}N]-ammonium chloride. The minimal medium(M- ^{15}N) used consisted of 6g/L Na_2HPO_4, 3g/L KH_2PO_4, 0.5g/L NaCl, 1.0g/L $^{15}NH_4Cl$, 0.4% glucose (w/v), 2mM $MgSO_4$, 0.1 mM $CaCl_2$ and 80 µl of 10% thiamine.

The procedure for protein expression was as follows; A 5 mL culture of BL21 (DE3)/pDAWD5-6 was grown to saturation in LB containing 30 µg/ml of kanamycin sulfate. The 5 mL culture was centrifuged and the cell pellet was resuspended in 2 L of M- ^{15}N in a 5L fermetor flask. The cells were grown at 37°C to an OD_{600} of 0.45, the point at which protein expression was induced by addition of 1 mM IPTG. The cells were harvested 4 h later. The protein was isolated by the freeze thaw method and purified by same methods used for the unlabeled protein. The double labeled protein, ^{15}N and ^{13}C labeled WD5-6, was produced by expressing the pDAWD5-6 recombinant plasmid in a media consisting of 6g/L Na_2HPO_4, 3g/L KH_2PO_4, 0.5g/L NaCl, 1.0g/L $^{15}NH_4Cl$, 0.4% 2mM $MgSO_4$, 0.1 mM $CaCl_2$, 80 µl of 10% thiamine and 0.4% ^{13}C- glucose (w/v) as the sole carbon source.

Determination of WD5-6 protein concentration

WD5-6 concentration was first determined by the Bradford protein assay (Biorad) and UV absorption methods. For the Biorad assay, a calibration curve was prepared by plotting increasing concentrations of immunoglobulin G (1.5 to 25 µg/mL) (IgG) versus the corresponding absorption at 595 nm. The resulting equation of the line was used to calculate the concentration of the purified WD5-6 protein. UV absorption measurement

was done at 276 and at 280 nm using molar absorptivity constant of 4350 $M^{-1}cm^{-1}$ and 4080 $M^{-1}cm^{-1}$ respectively. The molar absorptivity constants were derived from amino acid sequence analysis by the ProtParam program (Expassy website). Four μL of WD5-6 protein was diluted to 200 μL using 20 mM sodium phosphate, 6M guanidium chloride, pH 6.5 buffer in clean narrow path quartz cuvette. The UV absorption measurement was then taken at 276 and 280 nm. Concentration by the UV method was determined by equation 2.2 below.

$$c = \frac{A \times DF}{\varepsilon \times b} \qquad 2.2$$

Where c is the protein concentration in moles per liter, A is the UV absorbance at a given wavelength, b is the light path-length in cm, DF is the dilution factor and ε is molar absorptivity constant.

Amino acid hydrolysis

Amino acid hydrolysis analysis of WD5-6 was performed at the Protein Chemistry Laboratory at Texas A&M to determine its exact concentration and composition. Two μL of WD5-6 stock solution was desalted and resuspended in 20 mM MES/Na, pH 6 before use in the experiment. Total amino acid hydrolysis was used to analyze WD5-6.

Isoelectric point determination

The isoelectric point (pI) of WD5-6 was determined using pH 3-9 gradient gels on a Pharmacia PhastSystem employing the Broad Range pI calibration kit from Amersham

Pharmacia Biotech. Isoelectric focusing consisted of three steps: a prefocusing step (2000 V, 2.5 mA, 3.5 W for 75 volt hours), a sample application step (200 V, 2.5 mA, 3.5 W for 15 volt hours and a focusing step (2000 V, 2.5 mA, 3.5 W for 410 volt hours. About 2 μg of protein was loaded. The broad range pI calibration kit from Amersham Pharmacia Biotech was used.

IEF gels were stained manually in four steps: (i) fixing the gel with 20% trichloroacetic acid for 10 min at room temperature, (ii) rinsing with 10% acetic acid and 30% methanol solution for 2 min at room temperature, (iii) staining with 0.02% Coomassie Brilliant Blue, 0.1% copper (II) sulfate, 10% acetic acid and 30% methanol at 50 ˚C for 20 min and (iv) destaining with 10% acetic acid and 30% methanol solution at 50 ˚C. The gel was air-dried then scanned. A standard curve was formed by plotting distance migrated by the standard proteins versus their pIs. The resulting equation of the line was used to calculate the pIs of samples based on the distance they migrated in the gel.

Determination of the MW and aggregation status of WD5-6

MW and aggregation status of WD5-6 were determined by mass spectrometry, high resolution gel filtration and laser light scattering methods.

MALDI mass spectrometry

Matrix Assisted Laser Desorption Ionization (MALDI) mass spectrometry was used to determine the molecular mass of WD5-6 at Michigan State University. Two μL of

purified W5-6 solution (0.9 mM) was used for the experiment. The mass spectrometry experiment was done using a JEOL AX-505 double focusing mass spectrometer.

High resolution gel chromatography (HRGC) analysis

Apparent MW and aggregation status of WD5-6 were determined by HRGC analysis and HPLC size exclusion laser light scattering. A calibration curve was prepared by (i) measuring the elution volumes of standard proteins; Ribonuclease A (MW = 13,700 Da), Chymotrypsinogen A (MW = 25,000 Da), Ovalbumin (MW = 43,000 Da) and Albumin (MW = 67,000 Da), (ii) calculating their corresponding K_{av} (elution parameter) values and (iii) plotting their K_{av} values versus the logarithm of their molecular weight. Fifty µL of 164 µM apo-WD5-6 was reduced by addition of 10 mM DTT, incubated on ice for 10 min, and then injected into a HR 10/30 column (Amersham Pharmacia Biotech). WD6 was used as a control.

The HRGC column, Superdex G 75 10/30 (Pharmacia), was pre-equilibrated with 20 mM MES/Na, pH6, 150 mM NaCl and 10 mM DTT buffer. The sample was eluted in same buffer as the standards at a flow rate of 0.5 mL/min. The retention volume was then compared to a calibration curve previously prepared. Dextran Blue 2000 dye was used to determine the void volume (V_o) of the column.

Laser light scattering of WD5-6

Most of the methods used to characterize the WD5-6 protein required accurate determination of its MW and aggregation status. Theoretically, the amount of laser light scattered is proportional to the product of molecular mass of the protein and its

concentration (mg/mL) in laser light scattering experiment. Molecular weight (MW) and aggregation status of WD5-6 was determined by a high performance liquid chromatography (HPLC) size exclusion laser light scattering experiment that was done at the Yale Keck Biophysics Facility. The Superdex 75 HR 10/30 column (Pharmacia) for size exclusion chromatography was connected on-line with the following detectors; a Waters 996 Photodiode array multi-wavelength UV/VIS detector (Waters), a DAWN-DSP LS detector (Wyatt Tech.) and an OPTILAB DSP RI detector (Wyatt Tech.). The system was calibrated using 5 proteins (cytochrome c, Carbonic anhydrase, ovalbumin, bovine serum albumin and alcohol dehydrogenase) whose MWs extend from 12.4 kDa to 147 kDa.

The MW of WD5-6 was determined from the absolute measurement of scattered light intensity measured at 18 different angles. Comparison of the UV/RI signal ratio across the peaks of interest provided information relating to the homogeneity of the sample. Measurement was done at two concentrations and MW was calculated using ASTRA software.

Metal binding and transfer experiments

These experiments were performed to establish the copper: WD5-6 binding stoichiometry and whether copper transfer can occur between WD5-6 and WD4. In determining binding stoichiometry, two methods were used; (i) titrating a Cu(I) solution into a WD5-6 solution containing a reducing agent and (ii) metallation of a known amount of protein with Cu, washing the unbound Cu in an Amicon ultra-filtration device

then running on HRGC column. The peak fraction was collected and analyzed for Cu and protein content by Biorad protein assay and ICP-MS respectively.

Preparation of 1 M sodium phosphate buffer, pH 7.2

The sodium phosphate buffer was prepared by mixing 140 mL of 2 M monobasic phosphate solution with 360 mL of 2 M dibasic phosphate then diluting to 1L with distilled water (dH_2O). Two molar monobasic phosphate was prepared by dissolving 69 g of monohydrate sodium phosphate (Formula weight, FW, = 137.99) in 160 mL of distilled water then the solution was brought to 250 mL with dH_2O. On the other hand, 2 M dibasic phosphate solution was prepared by dissolving 141.96 g of anhydrous disodium hydrogen phosphate (FW = 141.96 g) in 300 mL of dH_2O then bring it to volume with to 500 mL with dH_2O.

Preparation of 10 M guanidium chloride 0.1M sodium chloride solution

Guanidium chloride is the commonly used chemical to denature proteins in solution. Sodium chloride is included to enhance the ionic strength and to stabilize the denatured state of protein. One hundred mL of 10 M guanidium chloride (FW = 95.53 g), 0.1 M NaCl (FW = 58.44g) solution was prepared by dissolving 95.53 g of guanidium chloride and 0.5844 g of NaCl in 50 mL dH_2O then brought to volume with dH_2O.

Preparation of WD5-6 sample

Protein concentration was calibrated and estimated by the total amino acid hydrolysis data from Texas A&M. A known amount was measured out, reduced by addition of 4

fold DTT, degassed, filled back with nitrogen then transferred into a VAC vacuum atmosphere anaerobic chamber. The sample was exchanged in 0.1 M sodium phosphate buffer pH 7.2.

WD5-6 metal binding experiment

A portion of the WD5-6 sample prepared above was mixed with excess Cu (I) solution, incubated for 10 minutes and then exchanged in 0.1 M sodium phosphate buffer to get rid of excess metal. The final sample was brought out of anaerobic chamber and run on a Superdex G75 HR column. The peak fraction was collected and analyzed by ICP-MS for copper content. Protein concentration was determined by Biorad protein assay. Binding stoichiometry was estimated from the ratio of final protein and copper concentration. The experiment was done in triplicate.

Analytical gel filtration of WD5-6 and WD4

This preliminary experiment was done to establish the high resolution gel running properties of WD5-6 and WD4, and to gauge the suitability of using this method to monitor metal transfer between WD5-6 and WD4. WD5-6 has a MW of 16,049 D while WD4 has a molecular mass of about 7 KD and this is a good basis to separate them by HRGC. The Cu(I)WD5-6 and WD4 were prepared adding 10-fold DTT to a dilute (0.1-0.5 mM) protein solution in 0.1 M sodium phosphate buffer at pH 7.2 followed by 2 fold excess of $CuSO_4$ solution. The protein solution was concentrated and washed with buffer containing 2 mM DTT as appropriate to achieve a 2-fold DTT: protein ratio in the sample.

The HRGC column was first equilibrated using 20 mM MES/Na pH 6.0, 150 mM NaCl buffer. The samples were then injected into the column and run at a flow rate of 0.5 mL/min. Elution volumes were recorded. Three blank runs were done before actual samples to ensure the column was in good shape. Samples injected were apo and Cu (I) - WD5-6, apo and Cu(I)WD4, and a combination of WD5-6 and WD4. Both the apo and metallated proteins were run to ensure metallation doesn't shift the elution peak.

Circular dichroism experiment

A circular dichroism (CD) experiment was used to probe α-helicity of WD5-6. A WD5-6 solution was prepared by reduction in 100 mM DTT and then exchanging in 0.25 mM sodium phosphate, pH 7.2 buffer under anaerobic conditions. The final sample had a concentration of 1.56 μM WD5-6. A 10 mm jacketed cell was thoroughly cleaned and dried before samples were introduced. The spectropolarimeter was attached to a nitrogen generator flow from oxidation by atmospheric oxygen. Temperature was set and maintained at 25 ˚C by running water through a jacketed cell. After 1 hr of incubation the samples were scanned, starting with the blank, at a rate of 2 nm per second over the far UV range of 190 nm to 260 nm. CD spectra were collected on a J-715 spectropolarimeter (JASCO, Japan) fitted with a 150 W Xenon lamp. The spectrum was corrected for background noise.

Chemical unfolding experiment

This was a preliminary experiment done to determine the UV absorption and emission properties of WD5-6 and to establish whether emission spectroscopy can be used to study unfolding of this protein. An apo-WD5-6 sample was prepared by exchanging it with a 0.1 M phosphate buffer, pH 7.2 and then adjusting to a final concentration of 31.2 μM WD5-6. Five mM tris-(2-carboxyethyl)-phosphate hydrochloride (TCEP-HCL) was added to the final sample to keep it reduced. All the buffers, solutions and water used for this experiment were vacuum-filtered through a 0.22 μm membrane and covered to avoid dust contamination. The instrument was blanked with 0.1 M sodium phosphate buffer, pH 7.2.

Emission measurements

The samples were excited at 278 nm. A bandwidth of 5 nm was used both for excitation and emission. The emission spectrum was recorded between 290 nm and 400 nm. Different concentrations of guanidium chloride for the denaturing experiment were prepared as shown below (Table 1). The samples were first incubated for 20 min then measured starting with the blanks in the order of increasing concentration of guanidium chloride. The cell was thoroughly cleaned and dried before measurements begun. The cells were carefully rinsed between the measurements.

Samples	1 M Sodium phosphate buffer	10 M Guanidium chloride/0.1 NaCl	dH_2O	0.312 mM WD5-6	1 M TCEP.HCl
1	100	0	895	0	5
2	100	0	890	5	5
3	100	200	690	5	5
4	100	400	490	5	5
5	100	600	290	5	5
6	100	800	90	5	5

Table 1. Preparation of WD5-6 samples with different guanidium chloride concentration. The amounts are in μL of ingredients used in the fluorescence unfolding experiment. Sample 1 is the sodium phosphate buffer blank while the sample 2 is for the WD5-6 blank (without the denaturant).

NMR spectroscopy

The strategy used for the determination of solution NMR structure of WD5-6 involved careful preparation of unlabeled and labeled protein solutions, spectra acquisition, spins system and sequential resonance assignment, collection of conformational constraints and calculation of the 3D structure. Spin system resonance assignment identified which proton resonance belonged to which residue type while sequential resonance assignment showed which proton belonged to which residue in the WD5-6 protein sequence. The calculated NOE and J-coupling NMR constraints were used to identify which protons were close in space and what the torsion angles were. The structure calculated represents conformation(s) consistent with all the NOE, J-coupling and other constrains. The reported structure is a mean of an ensemble of 20 lowest energy structures of the protein calculated from the collected data.

NMR sample preparation

Protein sample preparation is a very important step in NMR experiments. The purity, MW and aggregation status of WD5-6 were confirmed by various methods described above. Six hundred and seventy µL of a 0.9 mM WD5-6 stock solution was aliquoted, reduced by addition of excess DTT, degassed, filled back with nitrogen, then transferred into a VAC anaerobic atmosphere nitrogen chamber. The sample was thoroughly degassed because oxygen is both paramagnetic and an oxidizing agent. Paramagnetic elements such as oxygen lead to broadening of the lines of the NMR spectrum. Being an oxidizing agent, oxygen may lead to formation of disulfide bonds and/or chemical damage of the protein. The sample was then desalted by exchanging in 0.1 M sodium phosphate buffer pH 7.2 using an Amicon device fitted with a YM-3 membrane to reduce the concentration of DTT to about 2 mM.

The protein solution was then concentrated to 540 µL. Sixty µL of deuterium oxide was added to make 600 µL of 1mM WD5-6 (10% D_2O) solution. The sample concentration was estimated by the Biorad protein assay before loading into high quality NMR tube. The tube was capped with septum cap, brought out of the anaerobic chamber, packed and shipped to CERM, Italy for NMR analysis. All these manipulations were carried out anaerobically in a glove box with de-oxygenated buffers and solvents. This procedure was repeated for single and double labeled WD5-6 samples. The final protein concentration was about 1 mM.

NMR experiments

All NMR experiments were performed at the Magnetic Resonance Center (CERM), University of Florence, Italy. WD5-6 NMR spectra were acquired on Avance 900, 800, 600 and 500 Bruker Spectrometers operating at a proton nominal frequency of 900.13 MHz, 800.13 MHz, 600.13 MHz and 500.13 MHz respectively. All 2D and 3D spectra were collected at 298 K, processed using the standard Bruker software (XWINNMR) and analyzed using the CARA program.

^{1}H, ^{15}N-Heteronuclear single quantum coherence (HSQC) experiment

The ^{1}H, ^{15}N- HSQC experiment is a two dimensional (2D) experiment with one ^{1}H frequency and one ^{15}N frequency. Each of the naturally occurring amino acids (except proline) gives one signal on ^{1}H, ^{15}N- HSQC spectrum which corresponds to the N-H amide group. The ^{1}H, ^{15}N-HSQC experiment correlates the nitrogen atom of an NH_x group with the directly attached proton. Each signal in a HSQC spectrum represents a proton that is bound to a nitrogen atom. The spectrum contains the signal of the H^N protons in the protein backbone and since there is only one backbone H^N per amino acid, each HSQC signal represent one single amino acid.

NMR Titrations of WD4 and WD5-6 domains

These experiments were performed to monitor transfer of copper from Cu(I)WD4 and Cu(I)Atox1 to WD5-6. ^{15}N labeled apoWD5-6 was titrated with unlabelled Cu(I)WD4 and unlabeled Cu(I)Atox1 separately using NMR spectroscopy to follow the ^{15}N-^{1}H spectral changes upon addition of the unlabelled metallated protein partner.

Small amounts of metallated unlabeled proteins were added to the labeled samples in the NMR tube using a Hamilton syringe. Additions were done in a Coy chamber under nitrogen atmosphere at 298 K. The metallation of WD5-6 was monitored through ^{15}N-^{1}H spectral changes of valine 19 and valine 95 residues.

Resonance assignment and structural restraints

^{1}H - ^{1}H distances and the dihedral angles (φ and ψ) were determined through nuclear overhauser effects spectroscopy (NOESY) and HNHA experiments. H-bond constraints were obtained using transverse relaxation optimized spectroscopy (TROSY) version of the long range HNCO experiment at a magnetic field of 800 MHz. Relaxation experiments were performed on a Bruker Avance 600 MHz NMR at 298 K. The WD5-6 structure and folding was calculated from the constraints derived from these experiments.

Relaxation rate measurements

The Relaxation experiments were performed on Bruker Avance 600 MHz or 500 MHz spectrometers at 298 K. ^{15}N R_1, R_2, and steady-state heteronuclear ^{1}H-^{15}N NOEs were measured with pulse sequences as described by Farrow et al [51]. Integration of cross peaks for ^{15}N R_1, R_2, and ^{1}H-^{15}N NOEs spectra was performed by using the standard routine of the XWINNMR program. Relaxation rates R_1 and R_2 and heteronuclear NOE values were determined following a standard procedure as reported previously (Arnesano *et al.*, 2001). The experimental relaxation rates were used to map the spectral density function values, $J(\omega_H)$, $J(\omega_N)$, $J_{eff}(0)$, following a procedure available in literature (Peng & Wagner, 1992), in order to investigate the backbone motions (Peng & Wagner, 1992). An

estimate of the overall rotational correlation time was derived from the measured R_2/R_1 ratio by using a standard procedure (Kay *et al.*, 1989; Pervushin *et al.*, 1997)

CHAPTER III

RESULTS

Cloning of WD5-6

The portion of the WDP gene encoding for the N-terminal metal binding domains 5 and 6 (residues 485-633) was amplified from a human cDNA plasmid encoding full length WDP through 28 PCR cycles in a MiniCycler (MJ Research) employing Deep Vent DNA polymerase (New England Biolabs). The human cDNA plasmid was generously donated by Dr. Gitlin of Washington University, St. Louis, Missouri. PCR products were purified, double digested with restriction endonucleases Nco1 and BamH1 then cloned into an *E. coli* expression vector, pET24d+. The recombinant plasmid was maintained in DH5α cells.

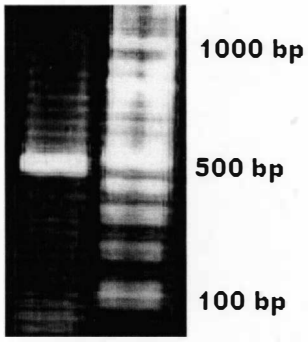

Figure 6. Agarose gel electrophoresis of WD5-6 recombinant plasmid digests on a 1.5 % gel. In lane1, is a band of the WD5-6 gene from a recombinant plasmid digestion (500 bp), in lane2, 100 bp marker.

Cloning was verified by sequencing of the gene in Dr. Barkman's lab and also by restriction analysis of the recovered plasmid employing BamH1 and BglII restriction enzymes. The sequence of the insert matched perfectly with the native sequence for this

portion of the gene. The alignment was done using the DNA Strider program. Band representing a fragment of DNA slightly below 500 base pairs (bp) was seen on a 1.5% agarose electrophoresis gel of the doubly digested recombinant plasmid (Figure 6). This confirmed that DNA of the right size was successfully inserted into the expression vector, pET24d+.

Induction of WD5-6 in LB media

The time course induction of WD5-6 protein was done to test whether WD5-6 could be efficiently expressed in LB media containing 30 μg/L of kanamycin. The recombinant plasmid was transformed into *E. coli* [BL21 (DE3)] cells and induced for WD5-6 protein expression in LB medium. Kanamycin was used to select for cells transformed with the recombinant plasmid because the plasmid contained genes for kanamycin resistance. The growth of the cells was monitored by measuring optical density at 600 nm (OD_{600}). WD5-6 expression was induced at OD_{600} of 0.45 by addition of 1 mM IPTG. IPTG binds and inactivates the lac operon repressor and hence induce WD5-6 gene transcription by RNA polymerase. The OD_{600} reading was taken every 30 min for 4 hours after induction and each time a 0.5 mL sample was withdrawn, centrifuged and analyzed on SDS-PAGE gel for WD5-6. The loading on SDS-PAGE was normalized by the OD_{600} reading using equation 3.1.

$$\frac{OD_{600} \text{ at time } 0 \times 15\ \mu l}{OD_{600} \text{ at time } t_i} \qquad 3.1$$

The results showed a steady increase in cell density with time as was reflected by the OD_{600} (Table 2). This indicated that the bacterial cells growth was not hampered by addition of IPTG. The normalized loading on SDS-PAGE showed increase in intensity, with time, of a protein band of about 16 kDa believed to be of WD5-6 protein (Figure 7). This is a clear indication that induction and the expression system for WD5-6 worked well. A 10 L batch was planned to produce WD5-6.

Time (min)	OD_{600}	Normalized loading(μL)
0	0.4752	15
30	0.7086	10.1
60	0.8325	8.6
90	0.9667	7.3
120	1.0700	6.7
150	1.1900	6.0
180	1.2730	5.6
210	1.3560	5.3
240	1.4040	5.1

Table 2. Time course induction of WD5-6 protein showing steady increase in OD_{600} with time. The last column shows the amounts normalized by OD_{600} for loading on SDS-PAGE.

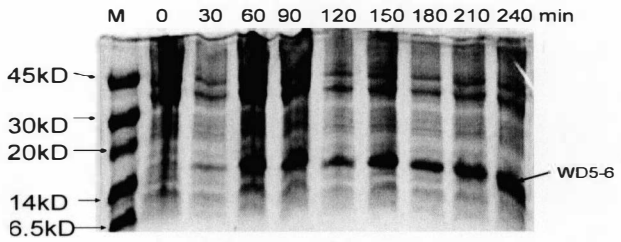

Figure 7. SDS-PAGE gel for time course induction of WD5-6 protein. The WD5-6 band of 16 kDa increases steadily with time. M is the Rainbow protein marker (RPN 755)

WD5-6 10 L batch production

Having shown that the WD5-6 protein is efficiently expressed by the designed WD5-6 expression system, a 10 L batch was produced in LB media containing same concentration of kanamycin following the protocol outlined earlier. The aim was to produce WD5-6 protein in sufficient quantities for characterization. The cells were pelleted by centrifugation then used for WD5-6 protein extraction by the freeze-thaw method. After harvesting and extraction, the WD5-6 crude extract was analyzed by SDS-PAGE. A strong band on SDS-PAGE gel of about 16 kDa, which is molecular mass of WD5-6, showed that WD5-6 protein was expressed well in the 10 L batch (Figure 8).

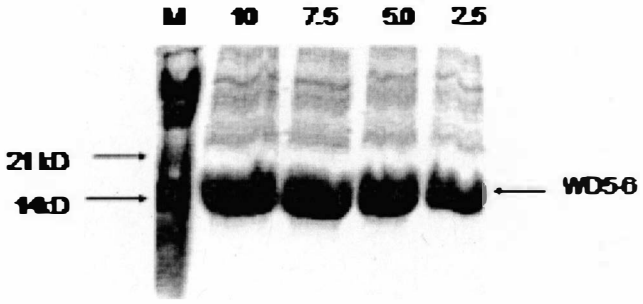

Figure 8. Tricine SDS-PAGE (15%) of freeze-thaw extracted WD5-6. Lanes 1; M is protein markers, 10, 7.5, 5.0 and 2.5 are different amounts (in μL) of WD5-6 extract loaded on the gel.

WD5-6 purification

WD5-6 was successfully extracted using the freeze-thaw method and isolated by a two step purification scheme involving anion exchange chromatography and gel filtration chromatography.

Ion exchange chromatography (IEC)

The WD5-6 extract was filtered then loaded onto a pre-equilibrated DEAE-Sepharose CL-6B anion exchange column (Amersham Pharmacia Biotech) in order to isolate it from the other contaminating proteins. Proteins that bear negative charge at pH 6 bind to the positively charged DEAE resin while the neutral and positively charged ones flow through without binding. The degree to which each protein binds to the column partially depends on the charge on the protein. Those that bind weakly are eluted first at low ionic strength while those that bind strongly are eluted at higher salt concentrations. WD5-6 has a pI of 4.87 and therefore bears net negative charge at pH 6 (pH of the buffer) and was expected to bind to the DEAE Sepharose anion exchange column.

Protein elution was monitored by the UV absorption profile at 254 nm. Polypeptides absorb UV light strongly around this wavelength. The resulting fractions were also analyzed by Biorad protein assay to identify protein containing fractions and also to estimate protein concentration (Table 3). SDS-PAGE analysis was used to identify WD5-6 containing fractions (Figure 9). SDS-PAGE separates proteins based on size; the smaller proteins experience less resistance in moving through the gel pores compared to the larger ones and therefore move faster through the gel. To estimate the protein sizes

more accurately, a set of protein standards of know MW were also ran alongside the samples.

IEC Fraction number	Absorbance at 595 nm	Concentration (μg/mL)
35	0.1718	229.3
39	0.3858	506.87
41	0.6176	807.52
46	0.8306	1083.8
50	0.7809	1019.3
52	0.8036	1048.8
59	0.2881	380.16
71	0.0348	51.62

Table 3. Biorad protein assay for IEC fractions. The left column shows IEC fraction numbers, the middle column show absorbance of fractions at 595 nm, while the right column show the protein concentration in μg/mL calculated from the IgG standard curve.

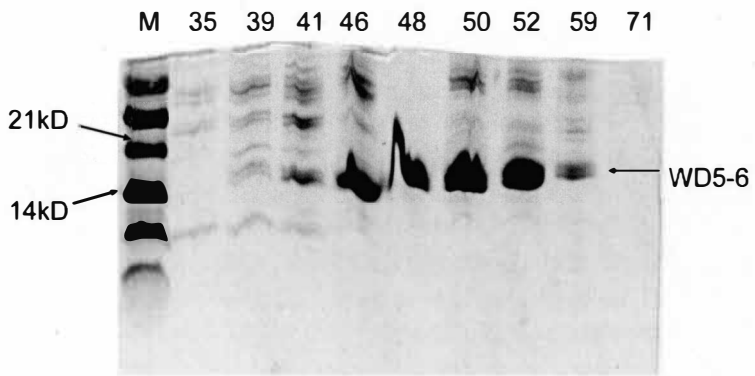

Figure 9. SDS-PAGE of IEC fractions. M is the Rainbow low molecular weight marker, 35-71 are IEC fractions. WD5-6 band of about 16 kDa is present in fractions 41-59.

The Biorad protein assay showed that all the peak fractions contained protein but at varied concentrations. Fractions 41 to 52 had the highest concentration. SDS-PAGE analysis was used to identify WD5-6 containing fractions. Five μl were withdrawn from each of the peak fractions, mixed with loading dye and water and run on a 15% Tricine SDS-PAGE gel (Figure 9). The gel revealed that WD5-6 eluted in fractions 41 through 59 which corresponded to about 30% salt concentration (0.3 M NaCl). The ion exchange chromatography concentrated WD5-6 in fractions 46-59 but the SDS-PAGE revealed the presence of other proteins of different molecular weights. To isolate WD5-6 further, a method which can separate proteins based on size was required.

Size exclusion chromatography (SEC) of WD5-6

This purification step was used to fractionate the proteins based on their sizes. The WD5-6 containing fractions from IEC were concentrated from 26 mL down to 2 mL using an Amicon device fitted with a YM3 membrane. The concentrated protein solution was loaded onto a Superdex G 75 10/30 gel filtration column(Amersham Pharmacia) pre-equilibrated with MES buffer (20 mM MES/Na, pH 6.0, 150 mM NaCl, 10 mM DTT).

SEC separates molecules based on size. Superdex G 75 separates molecules in the range of 3 to 75 kDa. In SEC, the larger molecules elute first while the smallest in column range elute last. UV absorption at 254 nm was used to monitor elution of proteins (Figure 10). Biorad protein assay was used to identify protein containing fractions. The WD5-6 containing fractions were specifically identified by SDS-PAGE. A single band of about 16 kDa appeared on SDS-PAGE column where fraction 36 was loaded (Figure 11).

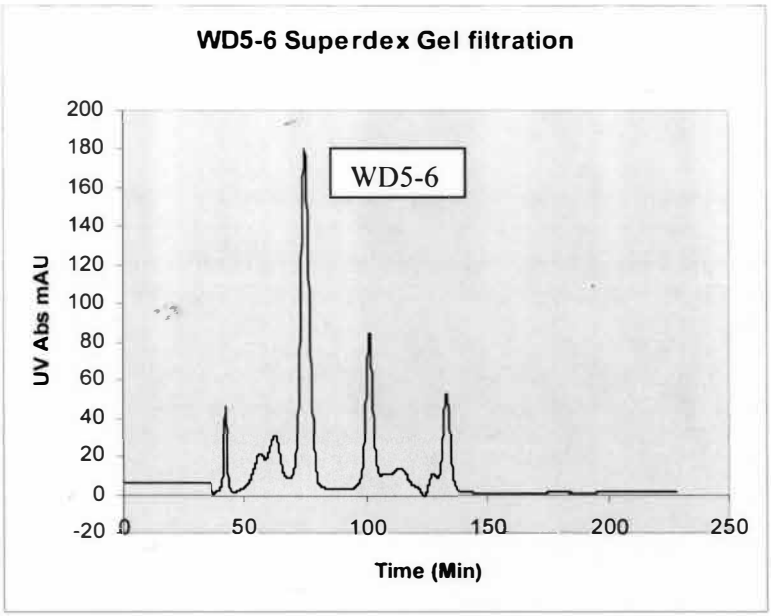

Figure 10. UV absorption profile of WD5-6 SEC elution. SDS-PAGE analysis revealed that the peak marked WD5-6 corresponding to fractions 35-39 contained the pure WD5-6 protein.

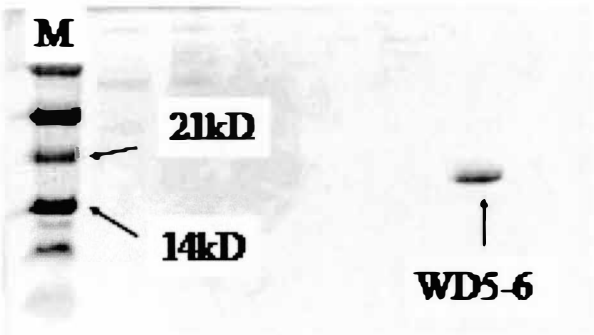

Figure 11. SDS-PAGE of SEC fractions. M is the molecular marker. WD5-6 band is shown on lane 7 where fraction 36 was loaded.

Fractions 35 to 39 under this peak were pooled together and concentrated down using an Amicon device fitted with a YM3 membrane. The final WD5-6 concentration

was determined using the Biorad protein assay, UV absorption spectrophotometry and total amino acid hydrolysis.

Determination of the concentration of purified WD5-6

The purified WD5-6 concentration was determined by 3 different methods; the Biorad protein assay, the UV absorption method and the amino acid hydrolysis method. For the Biorad assay an IgG standard curve was prepared and used to calculate the concentration of the WD5-6 protein. The binding of Biorad dye to the basic residues, especially arginine, uniformly increases its light absorption at 595 nm. The equation of the line for IgG standard curve was used to calculate the concentration of WD5-6 samples measured in the same manner. Equation 2.2 was used to estimate WD5-6 concentration by UV absorption method. The concentration of purified WD 5-6 was found to be 0.51 mM by Biorad assay while the UV method revealed a concentration of 0.61 mM. This difference prompted use of total amino acid hydrolysis method to determine the concentration of WD5-6.

The total amino acid hydrolysis found the concentration of WD5-6 to be 0.50 mM based on the average of all the amino acid residues. The amino acid composition was consistent with that of WD5-6 for all the amino acids except aspartate, asparagines, glutamate, glutamine and cysteins (Table 4). The concentration determined by Biorad assay was consistent with that of amino acid hydrolysis while that of UV absorption method overestimated the concentration by 22%.

AA		known # residues	predicted by AAA %AA	calculated from sequence % AA
ASX	115 1	11	7 6%	7 38%
GLX	129 1	19	12 8%	12 75%
SER	87 1	9	6 1%	6 04%
HIS	137 2	2	1 2%	1 34%
GLY	57 1	10	7 2%	6 71%
THR	101 1	8	5 2%	5 37%
CYS	103 2	5	1 9%	3 36%
ALA	71 1	17	11 8%	11 41%
ARG	156 2	3	2 8%	2 01%
TYR	163 2	3	2 0%	2 01%
VAL	99 1	9	6 1%	6 04%
MET	131 2	5	3 0%	3 36%
IS(1)				
PHE	147 2	5	3 4%	3 36%
ILE	113 2	17	10 1%	11 41%
LEU	113 2	12	8 4%	8 05%
LYS	128 2	9	7 1%	6 04%
IS(2)				
PRO	97 1	5	3 4%	3 36%
	Sum:	149	100%	100%
	Total residues in sequence:	149		

Table 4. WD5-6 total amino acid hydrolysis result is consistent with its amino acid composition. IS(1) and IS(2) are internal standards.

Molecular mass of WD5-6

MALDI-MS of WD5-6

The molecular mass of WD5-6 was determined by Matrix-Assisted Laser Desorption Ionization – Mass Spectrometry (MALDI-MS) at Michigan State University. The theoretical MW of WD5-6 is 16,049.5 Da. The MW determined by MALDI-TOF was 16,095.34 Da and is possibly for WD5-6 plus 2 Na^+ adducts (Figure 12). The buffer in which WD5-6 was stored had 150 mM NaCl. This deviation of MW by 0.24% is, however, within accepted experimental error. The second peak at 15,961 Da represents the MW of WD5-6 minus MW of methionine, which is the first residue in the WD5-6

amino acid sequence. The methionine residue was probably cleaved during excitation of WD5-6. There is a peak at exactly half the mass of the parent peak and this represents the doubly charged WD5-6.

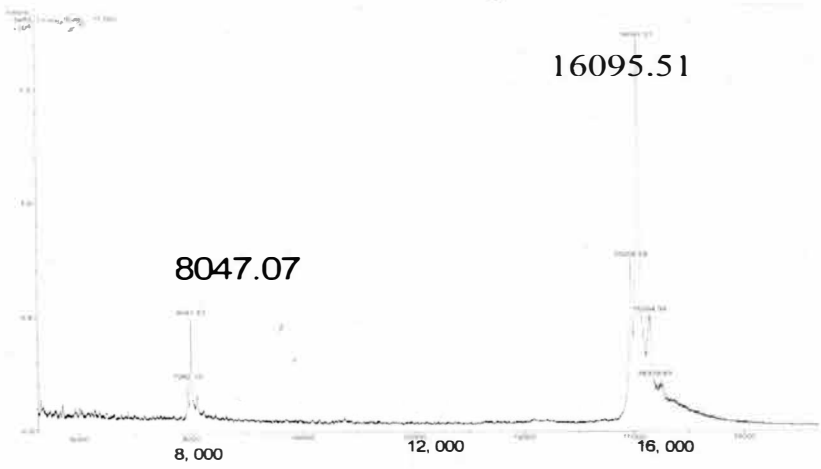

Figure 12. MALDI-MS spectrum of WD5-6.

High resolution gel chromatography (HRGC) results for WD5-6

The molecular mass and aggregation status of WD5-6 was determined by HRGC. A HRGC column was calibrated by running Dextran Blue 2000 to determine the void volume followed by four standard proteins with known MWs (Figure 13). The void volume (V_o) was found to be 8.2 mL. Total column volume (V_t) for this column is 23.56 mL. The K_{av} was calculated by the formula previously shown (Equation 2.3). WD5-6 and WD6 were run on the same column to determine their elution volumes that were used to calculate their K_{av} by equation 3.2 and molecular masses.

Elution parameter, $K_{av} = \frac{V_e - V_o}{V_t - V_o}$ 3.2

Where V_e = elution volume for the protein, V_o = Column void volume, V_t = total bed volume.

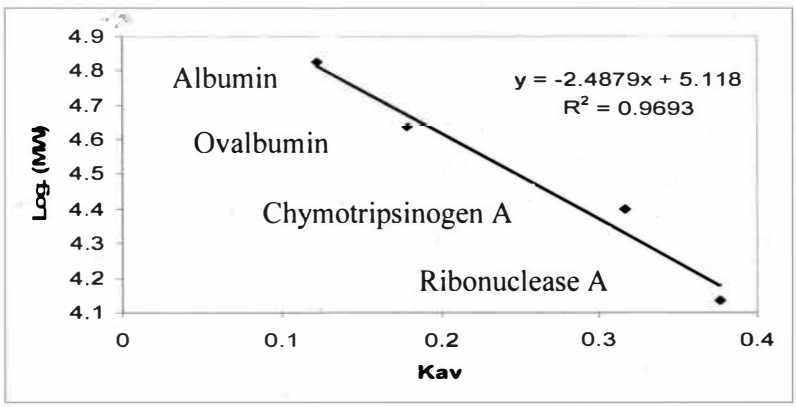

Figure 13. HRGC calibration curve. The elution parameter, K_{av} was plotted versus the logarithms of the MW of the standard protein to give a calibration curve from which the masses of the samples were calculated.

Sample	V_e(mL)	K_{av}	Apparent MW	Expected MW
WD5-6	12.65	0.2897	25,257	16,049
WD6	14.36	0.4	13,076	7,732

Table 5. Apparent running masses of WD5-6 and WD6 calculated from the HRGC.

The MW of WD5-6, as well as that of WD6, was overestimated by HRGC (Table 5). The apparent MWs were, however, less than those expected for dimeric forms of both the proteins. The elution profile of WD5-6 showed a single Gaussian peak (Figure 14). This showed that the WD5-6 solution is homogeneous and devoid of contaminants.

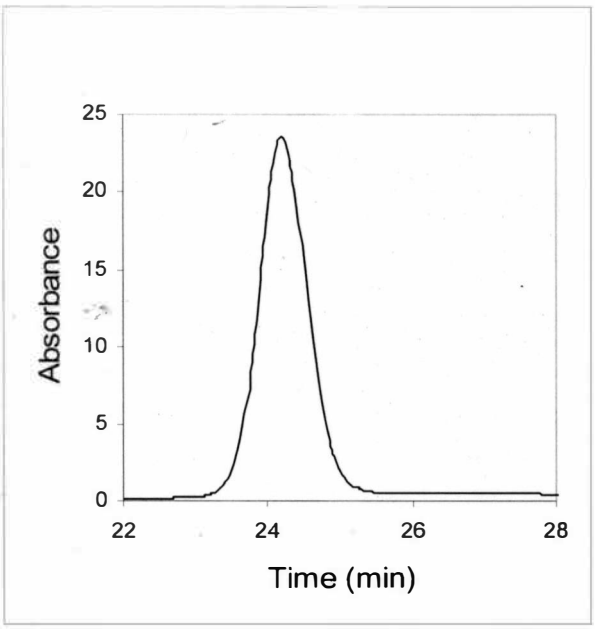

Figure 14. A WD5-6 elution peak from HRGC showing a single peak that eluted at 24.4 min at a flow rate of 0.5 mL/min.

Laser light scattering experiment

This experiment was done to determine the aggregation status and molecular mass of WD5-6. In this experiment, WD5-6 was first run on SEC column then detected by a laser light scattering and UV/RI detectors at the end of the column. The amount of light scattered is proportional to the product of size and concentration. The experiment was done in duplicate at different concentration. The results obtained (Table 6) showed two peaks which are clearly for WD5-6 monomer and dimer. The second peak of S1 run corresponded to the exact MW of WD5-6 (16.05 kDa) (Figure 15). WD5-6 dimer could have resulted from oxidation while the sample was on transit to Yale. The UV/RI ratio from the two peaks arising from different oligomers of WD5-6 remained unchanged for

the two peaks throughout the chromatogram. That was clear indication that WD5-6 was homogeneous

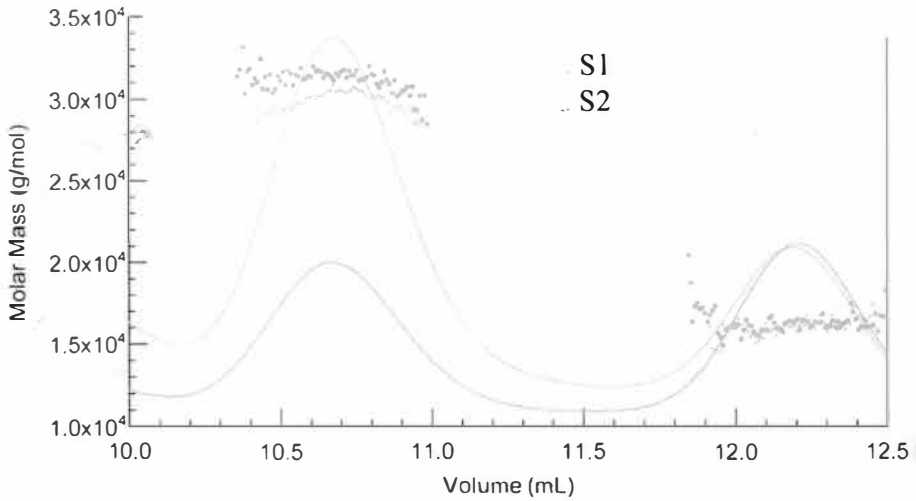

Figure 15. Plot of elution volume versus the molar mass of WD5-6. The S1 (green) and S2 (purple) are duplicates runs but S2 is at half the concentration of S1 sample. The ration of dimer to monomer is higher for S1 run and this could be due to higher concentration. More concentrated protein solution easily dimerize by formation of disulfide bonds. The molecular weight was calculated from data derived from the above plot by ASTRA software (Table 6).

Run	Peak Elution at UV trace (mL)	MW(kDa) Calculated by ASTRA (Average for the entire peak)	MW (kDa) Calculated by ASTRA range of MW observed	Sequence predicted MW for monomer (kDa)	Mono disperse peak
S1	10.60	29.92	29-31	16.05	Yes
	12.12	16.05	15-17	16.05	Yes
S2	10.60	31.22	30-32	16.05	Yes
	12.14	16.32	15-17	16.05	Yes

Table 6. The Laser light scattering results for WD5-6 protein showing two peaks for each trial. The monomer peak of S1 trial corresponds exactly to the MW of WD5-6. The MW corresponding to dimer was observed too for both trials.

Isoelectric point of WD5-6

This experiment was done to determine the isoelectric point (pl) of WD5-6 protein. A calibration curve was prepared by running standard proteins alongside WD5-6 sample and WD1 as a control. The pI for WD5-6 was calculated from the standard curve derived from a plot of the pI of standard proteins versus the distance migrated from the cathode on the isoelectric focusing gel. The distance migrated from the cathode in mm was measured from the dried isoelectric focusing gel shown below (Figure16).

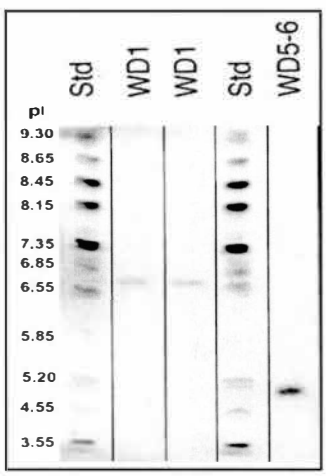

Figure 16. Isoelectric focusing gel. Lane 1 and 4, protein standards, lane 2 and 3, WD1 and lane 5, WD5-6. WD5-6 migrated 7.9 cm. WD1 was used as a control. WD1 was loaded at the cathode (lane2) and at the anode (lane3).

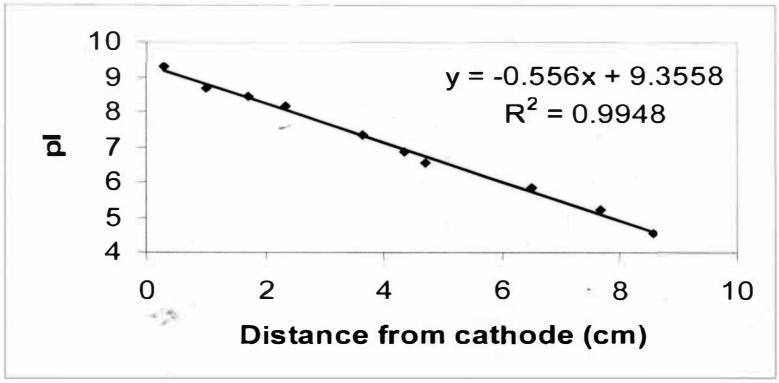

Figure 17. IEF calibration curve. Linear regression analysis of the standard curve (Figure 16) gave a best fit line with equation 3.3. Equation 3.3 gave a pI of 4.96 for WD5-6. The pI of WD5-6 predicted from the sequence is 4.87.

$$y = -0.5784x + 9.4181 \qquad 3.3$$

WDP domain one, WD1, that was previously isolated and characterized in our laboratory, was used as a control. WD1 migrated to the same pH both from anode and cathode. This showed that the gel was run under appropriate conditions. The determined pI of WD5-6 is consistent with the sequence predicted pI of 4.87.

WD5-6 – Cu binding results

This experiment was done to determine the Cu(I)-WD5-6 binding stochiometry. Cu(I) solution was added to WD5-6 solution in inert environment and then exchanged in 0.1 M sodium phosphate buffer in Amicon device to wash away unbound Cu. The resulting Cu(I)WD5-6 complex was then loaded and run on a preequilibrated HRGC column. A total of 5 mL covering the elution peak of Cu(1)WD5-6 complex from the

HRGC column was collected and analyzed for Cu and WD5-6 protein content. Protein concentration was estimated by Biorad protein assay while Cu concentration was determined by inductively coupled plasma mass spectrometry (ICP-MS). The average ratio of WD5-6: Cu was determined to be 0.479 ± 0.0287 (Table 7). This results showed that WD5-6 binds 2 equivalents of Cu(I) and is consistent with earlier evidence that showed that the 6 N-terminal metal binding domains of WDP bind up to 6 equivalents of Cu (DiDonato et al., 1997).

Trial	Cu concentration	WD5-6 concentration		WD5-6:Cu ratio
	(nM)	(μg/mL)	(nM)	
1	13.25	105.8	6.83	0.498
2	14.99	118.5	7.38	0.493
3	16.70	120.3	7.50	0.446

Table 7. Determination of WD5-6 and Cu concentrations in the Cu(I)WD5-6 complex by Biorad protein assay and ICP-MS respectively.

Analytical gel filtration results of WD5-6 and WD4

This experiment was done to determine the elution parameters of WD5-6 and WD4 on HRGC column. The HRGC was to be used to monitor Cu transfer from WD4 to WD5-6 proteins. WD4 was expressed and purified in a similar manner as WD5-6. The WD5-6 protein has a MW of 16.05 kDa while WD4 has a MW of 7.7 kDa and were therefore expected to elute at different volumes from HRGC column. Binding of Cu to Cu binding proteins enhances their extinction coefficients and this increase could be used to monitor Cu transfer from WD4 to WD5-6. Both proteins were loaded on HRGC column alone and together to determine their elution parameters before the actual Cu

transfer experiment. The apo and copper- loaded WD5-6 eluted at about 12.2 mL while the apo and copper loaded WD4 eluted at about 13.2 mL from HRGC column (Table 8). All the samples showed a single distinct UV absorption peak which indicated that they were homogeneous both in apo and metallated forms. The resolution was, however, poor between the WD5-6 and WD4 peaks when injected into the column simultaneously and that ruled out the possibility of using this method to perform metal transfer studies between the two domains. To accomplish metal transfer studies, peak fractions needed to be collected separately for both WD4 and WD5-6 to be analyzed for Cu and protein content.

Sample	Peak1 Elution volume (mL)	Peak 2 Elution volume (mL)
WD5-6	12.214	
WD4	13.240	
Cu(I)WD5-6	12.212	
Cu(I)WD4	13.220	
WD5-6, WD4	12.209	13.260

Table 8. Analysis of WD5-6 and WD4 protein samples by HRGC.

α -Helicity of WD5-6

This experiment was done to determine the α –helicity of WD5-6 protein. The WD5-6 sample was prepared in 0.01 M sodium phosphate buffer and used for this experiment. The measurements were taken at a spectropolarimeter at Michigan State University. The data got were corrected for background noise and used to calculate α – helicity of WD5-6.

The difference in absorption of left and right circularly polarized light yields an elliptically polarized beam that can be measured by the CD spectropolarimeter, which converts it into ellipticity by equation 3.4.

$$\Theta = [2.303(A_L - A_R)]/4l \qquad 3.4$$

Where Θ is ellipticity in millidegrees, l is the light path length through the cell and A_L and A_R are absorbencies for left and right circularly polarized light respectively. Millidegrees were converted to mean residue molar ellipticity by the equation 3.5.

$$[\Theta] = \Theta/10Cln \qquad 3.5$$

Where $[\Theta]$ is mean residue molar ellipticity in $deg.cm^2 \cdot dmol^{-1}$, C is the protein concentration in mol/liter and *n* the number of residues in the protein.

The α-helix presents a minimum signal at 222 nm (Figure 18). The CD signal at this wavelength was used to calculate α-helicity. The mean residue ellipticity for 100% helix at 222 nm is obtained by equation 3.6.

$$[\Theta]_{222} = 40{,}000(1-2.5/n) \qquad 3.6$$

Where *n* is the number of residues in the sequence (which is 149 for WD5-6).

The $[\Theta]_{222}$ for WD5-6 equaled -9097.14 while for 100% helicity is equal to -40269. Percent α-helicity for WD5-6 was therefore calculated to be 23%. This is consistent with the "ferrodoxine like" fold expected for P-type ATPase metal binding domains.

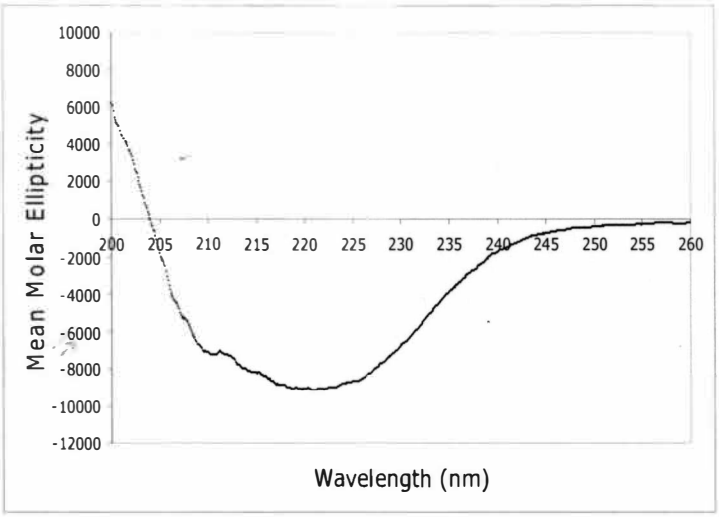

Figure 18. CD spectrum of apo-WD5-6 showing a minimum at 222 nm.

Chemical unfolding of WD5-6

This experiment was performed to show the unfolding characteristics of WD5-6. The WD5-6 protein was prepared in 0.01 M sodium phosphate buffer containing 5 mM TCEP.Cl. TCEP.Cl was added to prevent WD5-6 from oxidizing. Guanidium chloride was used to denature WD5-6 and the unfolding was monitored by emission spectroscopy at different denaturant concentrations. An excitation spectrum of WD5-6 showed a maximum at 278 nm (Figure 19), which is typical of Tyr excitation. The sample was excited at 278 nm and the emission was recorded from 290 nm to 400 nM. Tyr emission maximum usually occurs at 303 nm. The WD 5-6 protein has 3 Tyr residues but no Trp.

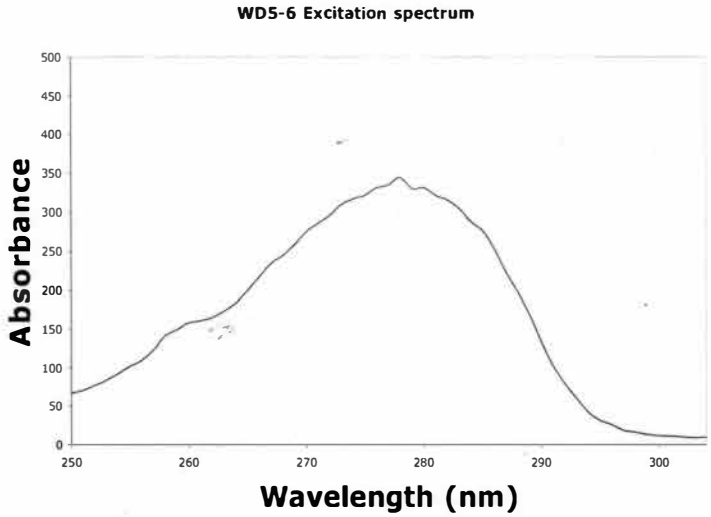

Figure 19. Excitation spectrum of WD5-6. The absorption maximum of about 280 nm is typical of Tyr excitation spectrum.

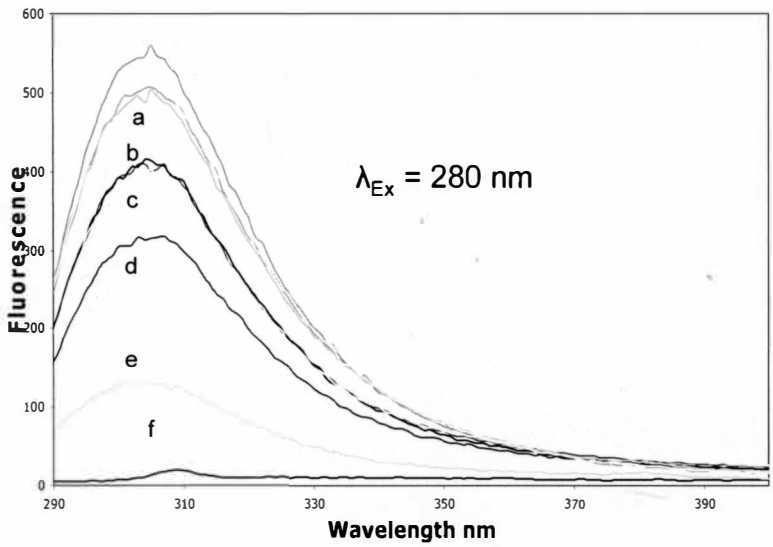

Figure 20. Unfolding plots of WD5-6 at different denaturant concentrations. (a) WD5-6, (b) 2 M (c) 4 M (d) 6 M (e) 8 M (f) Blank. 2 M to 8 M guanidium chloride was used to denature WD5-6

The excitation spectrum of WD5-6 reveals a peak at 278 nm (Figure 19) which is typical for Tyr absorption. Emission diminished with increasing concentration of guanidium chloride (Figure 21). WD5-6 emission is due to Tyr residues and the diminishing emission is due to change in the chemical environment due to unfolding.

NMR Results

The NMR experiments were done to elucidate the 3 dimensional structure of WD5-6, to monitor Cu transfer from Cu(I)WD4 and Cu(I)Atox1 to WD5-6 and to probe the dynamic of Wd5-6. All the NMR experiments were done at CERM, University of Florence, Italy.

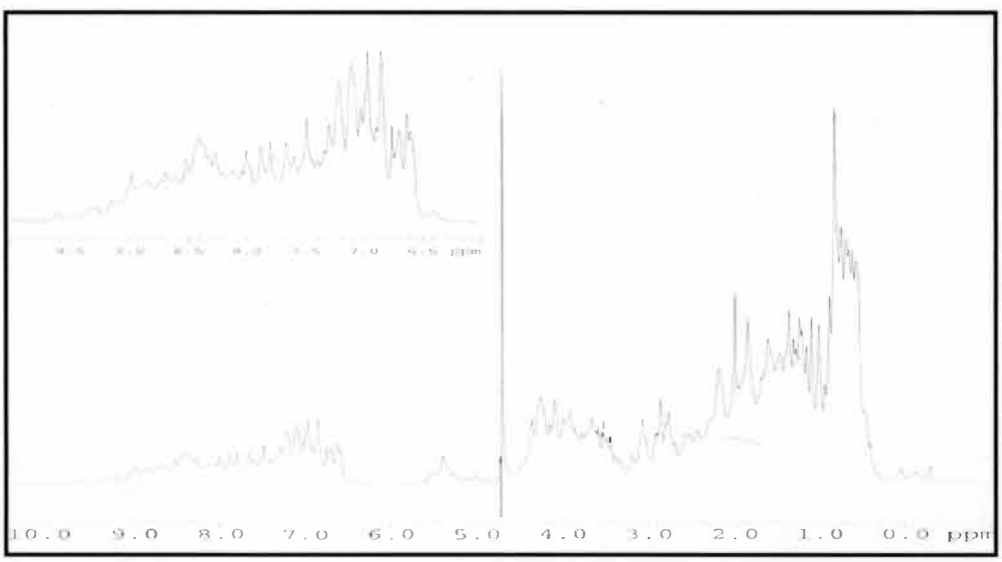

Figure 21. ^{1}H 1D NMR spectrum of WD5-6. The amide region (6.5-9.5) is expanded. The intensity and distribution of peaks seen on this spectrum is a good for NMR experiments.

The ^{1}H 1D NMR spectrum of WD5-6 (Figure 21) showed good peaks and generally showed that the protein solution was in stable condition suitable for NMR experiments.

^{1}H-^{15}N-HSQC spectrum of WD5-6

The folded protein or domains of protein displays broad distribution of NMR frequency resulting in a good spread-out of cross peak signals in the ^{1}H- ^{15}N HSQC. Unfolded proteins show heavy overlap of signals on the ^{1}H- ^{15}N HSQC spectrum. WD5-6 is well folded according to the 2D ^{1}H -^{15}N HSQC spectrum (Figure 22). Assignment of the ^{1}H- ^{15}N HSQC spectrum is consistent with the WD5-6 protein sequence. The distribution of signals is crucial for further structural determination and copper binding experiments.

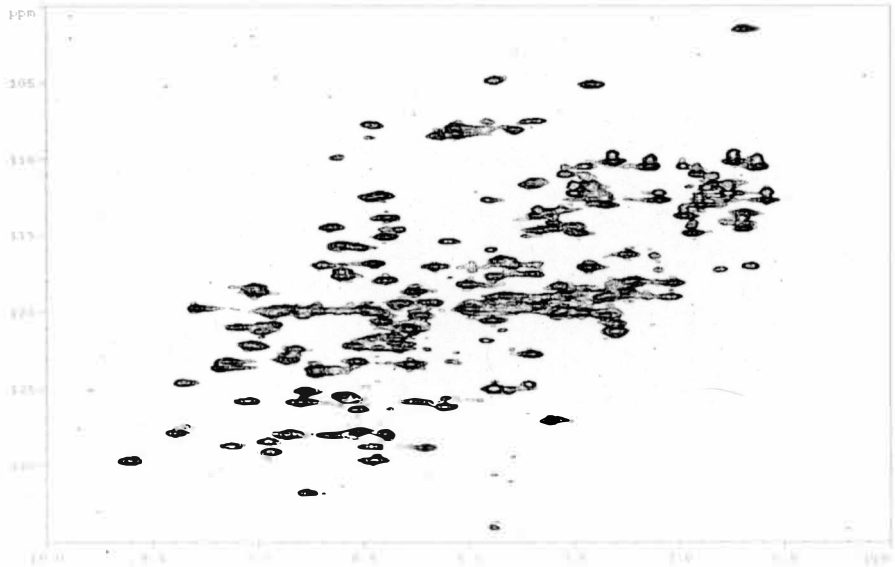

Figure 22. The ^{1}H-^{15}N HSQC spectrum of WD5-6.

Cu(1) - WD5-6 ^{1}H- ^{15}N HSQC NMR titration

The ^{1}H- ^{15}N HSQC NMR spectroscopy was used to monitor Cu(1) binding to WD5-6. Cu(I) was titrated into labeled WD5-6 protein solution using Hamilton syringe in Coy chamber under nitrogen atmosphere at 298 K. Upon addition of Cu(I), shifting of cross peak signals indicate residues that experience a change in their environment (chemical exchange). The copper binding to WD5-6 produced spectral changes limited to the two copper binding regions and did not affect its aggregation state as well as the overall structural properties, in particular without triggering changes of the relative orientation of the two subunits (Figure 23). This aspect of the ^{1}H- ^{15}N-HSQC experiment was utilized during the titration of Cu (I) loaded unlabelled WD4 and Atox1 proteins into the labeled apo-WD5-6 protein solution.

Cu(1)WD4 - WD5-6 ^{1}H- ^{15}N HSQC NMR titration

The ^{1}H- ^{15}N HSQC NMR spectroscopy was also used to monitor Cu(I) transfer from unlabeled Cu(I)WD4 and Cu(I)Atox1 to labeled apoWD5-6. The ^{1}H- ^{15}N spectral changes upon addition of increasing amounts of the unlabelled protein partner were monitored. The metallation of WD5-6 was monitored through residues Val 19 and 95, which are next to Cu(I) binding Cys 18 and 94 respectively, and thus showed a large chemical shift difference between the apo and Cu(I) loaded forms (Figure 24). Another advantage of using these two Val residues was that their NHs cross peaks were not overlapped in the ^{1}H - ^{15}N HSQC maps of apo and Cu(I) loaded forms of WD5-6. This allowed for easy integration during the titration stages. (Figure 24).

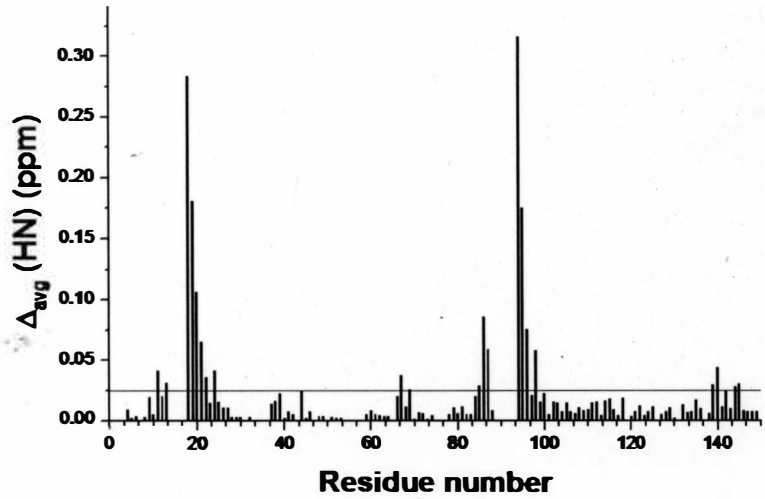

Figure 23. The weighted chemical shift difference δavg(HN). {[(δH)2 + (δN/5)2]/2}1/2 where δH and δN are chemical shift difference for 1H and 15N, respectively. Chemical shift differences are not reported for residues 14-17 and 90-93 as their 1H-15N cross-peaks are not observed for apo and Cu(I) forms.

The titration of Cu(I)WD4 into labeled WD5-6 resulted in Val 19 and Val 95 spectral shifts (Figure 24) indicating an interaction that led to Cu(I) transfer from WD4 to WD5-6, first to WD6 then to WD5 without formation of an adduct. Titration of Cu(I)Atox1 with WD4 showed formation of an adduct that is in fast exchange on the NMR timescale as confirmed by relaxation measurements. However, the behavior was dramatically different when Cu(I)Atox1 was titrated into labeled WD5-6. No Cu transfer occurred from Cu(I)Atox1 to WD5-6 and no stable adduct was formed between the two proteins even when an excess of Cu(I)Atox1 was added (Cu(I)Atox1:WD5-6 ratio of 2.5:1.0). This observation is consistent to the yeast two hybrid data that showed that Atox1 doesn't interact with WD5-6 (van Dongen et al., 2004).

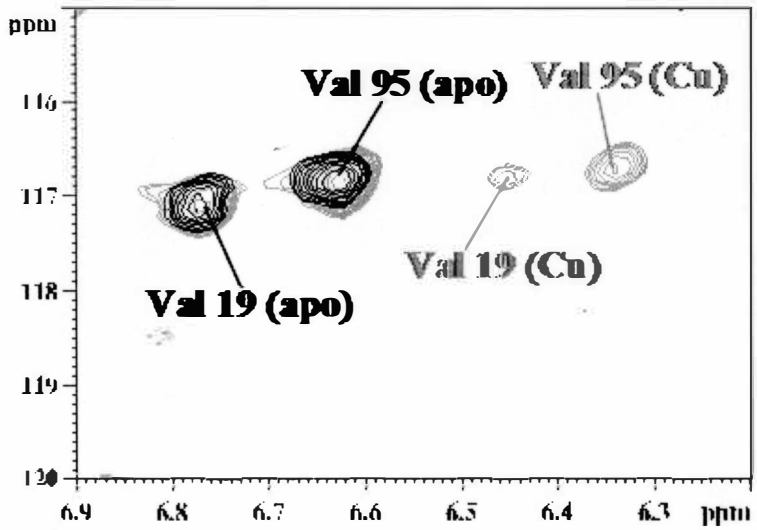

Figure 24. Superposition of ^{1}H - ^{15}N HSQC spectra of apoWD5-6 (black) and Cu(I)WD5-6 (red) showing simultaneous chemical shifts of Val 19 and Val 95.

Solution NMR structure of WD5-6

The secondary structure of WD5-6 derived from solution NMR structure show that each of the domains bears a ferrodoxine-like structure, βαββαβ (Figure 25). Analysis of WD5-6 NMR data revealed the following secondary structural elements; β1(4-11),α1(18-27), β2(34-38), β3(43-49), α2(56-64), β4(67-70), β5(81-86), α3(94-103), β6(109-114), β7(119-125), α4(132-140), β8(144-147) (Figure 25). The Cys 15 and Cys18 which coordinates copper in MBD5 are located at the first loop and first α-helix regions respectively while Cys 91 and 94 which coordinates copper in MBD6 are located in the first loop and first α-helix respectively.

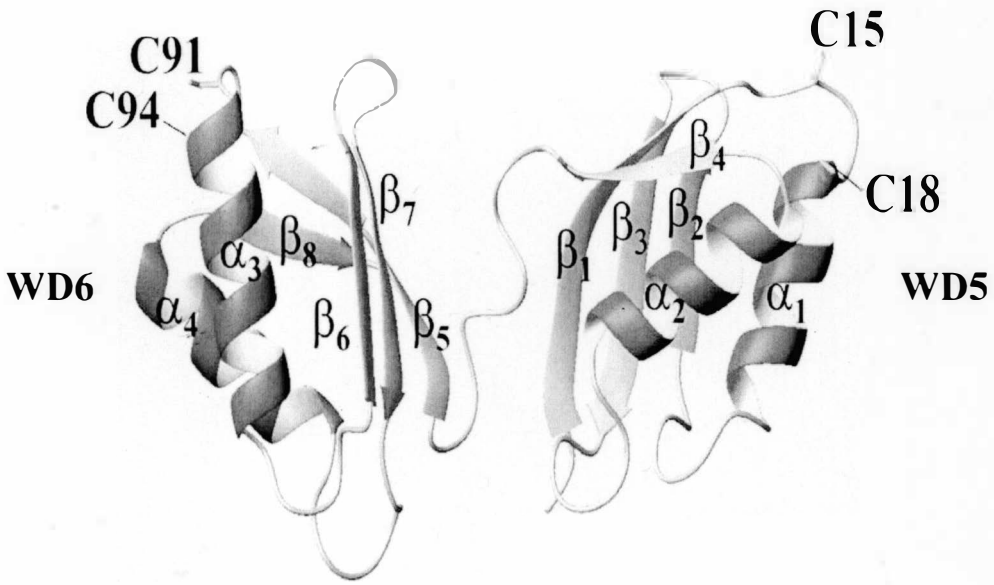

Figure 25. Ribbon diagram representative of the 20 lowest energy conformers of apo WD5-6. C15, C18, C91 and C94 are the Cu binding residues.

The acquired parameters for NMR experiments performed on WD5-6 (Table 9) were used to calculate constraints used to elucidate 3D structure of WD5-6. (Figure 25). ^{1}H, ^{15}N and ^{13}C resonance assignments of human apoWD5-6 at 298 K in 0.1 M sodium phosphate buffer, pH 7.2 with 2 mM are available upon request.

Experiments[a]	Dimension of acquired data (nucleus)			Spectral width (ppm)			n[b]
	t_1	t_2	t_3	F_1	F_2	F_3	
[^{1}H-^{1}H]-NOESY	1024(^{1}H)	2048(^{1}H)		15	15		64
[^{1}H-^{1}H]-TOCSY	1024(^{1}H)	2048(^{1}H)		15	15		64
[^{1}H-^{15}N]-HSQC	256(^{15}N)	1024(^{1}H)		40	7		8
[^{1}H-^{13}C]-HSQC	512(^{13}C)	1024(^{1}H)		70	15		8
CBCA(CO)NH	128(^{13}C)	48(^{15}N)	1024(^{1}H)	80	40	15	8
CBCANH	128(^{13}C)	48(^{15}N)	1024(^{1}H)	80	40	15	16
HNCO	96(^{13}C)	48(^{15}N)	1024(^{1}H)	16	40	15	8
HN(CA)CO	96(^{13}C)	48(^{15}N)	1024(^{1}H)	16	40	15	16
^{13}C (H)CCH-TOCSY	272(^{13}C)	96(^{13}C)	1024(^{1}H)	88	88	15	8
Long-range HNCO[c]	128(^{15}C)	1024(^{1}H)		16	15		1024
^{15}N-edited [^{1}H-^{1}H]-NOESY	256(^{1}H)	48(^{15}N)	1024(^{1}H)	15	40	15	16
^{13}C-edited [^{1}H-^{1}H]-NOESY	272(^{1}H)	96(^{13}C)	1024(^{1}H)	15	86	15	8
HNHA	128(^{1}H)	48(^{15}N)	1024(^{1}H)	15	40	15	16
HNCA	128(^{13}C)	48(^{15}N)	1024(^{1}H)	45	40	15	8
HN(CO)CA	128(^{13}C)	48(^{15}N)	1024(^{1}H)	45	40	15	8
$^2J_{NH}$ [^{1}H-^{15}N]-HSQC	256(^{15}N)	2048(^{1}H)		180	20		64

[a]All 3D and 2D spectra were collected at 298 K, processed using the standard Bruker software (XWINNMR). [b]Number of acquired scans.[c] A TROSY version of the long-range HNCO experiment were acquired at a magnetic field of 800 MHz for hydrogen bond detection.

Table 9. Acquisition parameters for WD5-6 NMR experiments performed on ***human*** apoWD5-6.

Relaxation rate measurements

Relaxation rate measurements were used to probe the dynamics of WD5-6 protein. The overall rotational correlation time (τ_c) of WD5-6 was found to be 9.1 ±0.6 ns, which is two times greater than that of WD6 alone (4.5 ns), and is the value expected for a monomeric protein of 16 kDa.

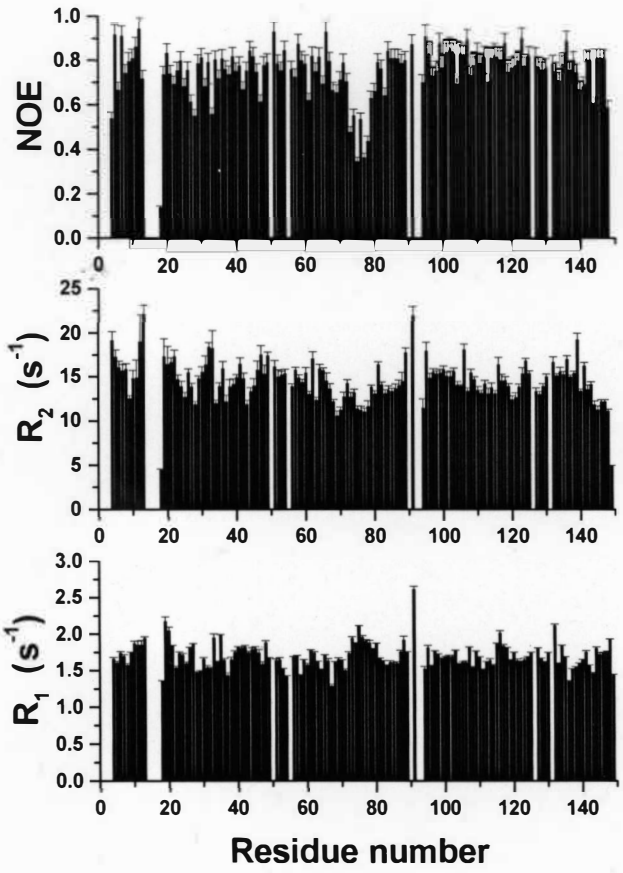

Figure 26. ^{15}N relaxation parameters R_1, R_2 and ^{1}H-^{15}N NOE versus residue number of apoWLN5-6 collected at 600 MHz.

Relaxation rate measurements also showed that WD5-6 reorients in solution as a single molecule (i.e. as a dumbbell) rather than as independent beads on a string, with essentially no relative reorientation of the two individual domains (Figure 26). Furthermore, the residues linking the two domains of apoWD5-6 did not experience conformational exchange processes on the ms-μs timescale (Figure 27) indicating the absence of a multiplicity of relative orientations of the two domains.

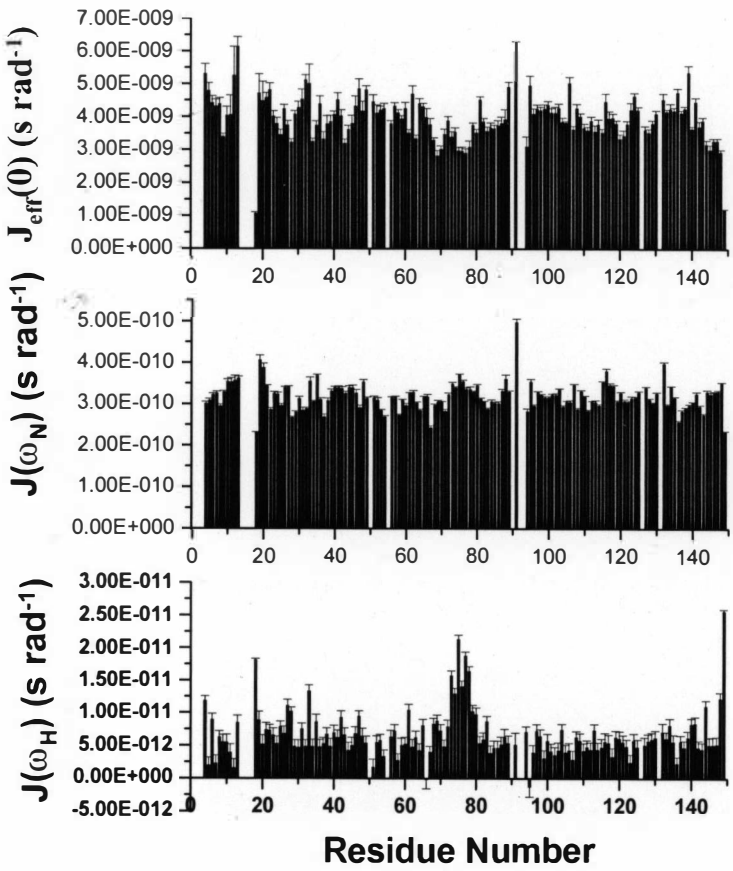

Figure 27. Spectral density function values for the $J(\omega_H)$, $J(\omega_N)$, and $J_{eff}(0)$ terms.

CHAPTER IV

DISCUSSION

The goals of this study were to clone, express, purify and characterize the multi domain construct of N-terminal metal binding domains 5 and 6 of Wilson's disease protein (WD5-6). The ability of this construct to bind copper and to accept copper from the fourth metal binding domain of the same protein was also probed. Elucidation of solution NMR structure of WD5-6 was also one of the goals of this study.

The gene encoding for WD5-6 was cloned into pET24d+ vector successfully and expressed well in *E. co*li as host cells. BL21 (DE3) cells were used because of their ability to encode the gene for tRNA of rare codons allowing for more efficient production of eukaryotic proteins that contain rarely used *E. coli* codons. A yield of 12 g/L of LB medium was realized for WD5-6. WD4 was also cloned into the same vector and expressed well in *E. coli* (BL21) cells. Both were extracted by the freeze thaw method and purified to homogeneity by two steps including anion exchange chromatography using a weak anion exchanger, DEAE-Sepharose, and size exclusion gel chromatography. The purified protein was characterized by various methods including; high resolution gel filtration chromatography, MALDI-TOF mass spectrometry, laser light scattering, isoelectric focusing, amino acid hydrolysis and spectroscopic techniques such as UV-Vis absorption spectroscopy, fluorimetry, CD and NMR spectroscopy.

The purification scheme used for WD5-6 was successful. IEC fractions that had higher protein concentrations according to the Biorad protein assay (Table 4) also contained WD5-6 as is evident on SDS-PAGE (Figure 9). This showed the success of this

purification technique. These fractions, however, had some higher and lower molecular weight proteins which necessitated the use of a different technique that could separate proteins based on their sizes. Size exclusion chromatography was used to further purify the IEC product to homogeneity (Figure 10).

UV absorption spectroscopy and Biorad protein assay are the common methods for estimation of protein concentration. The UV absorption method, however, over-estimated the WD5-6 concentration. The molar absorptivity of WD5-6 used assumed it was fully reduced. The molar absorptivity coefficients of reduced and oxidized proteins are different. DTT absorbs UV light at around 280 nm so it could not be used during the measurement and WD5-6 could have been oxidized resulting in this error.

WD5-6 migrates at a higher mass on HRGC column than the expected MW but less than the dimer MW. It's safe to conclude that it's monomeric because its apparent mass is roughly twice the mass of WD6 that was run as a control on the same gel. One possible reason why HRGC overestimated the MW of WD5-6 is that WD5-6 may not be as globular (spherical) as the standard proteins used to calibrate the gel. The apparent molecular mass derived from HRGC is a function of molecular mass and shape therefore the difference in size of the proteins could make them run differently on gels. WD5-6 and WD4 couldn't be completely separated by use of high-resolution gel chromatography. Consequently, metal transfer studies between them cannot be accomplished by this method. These two proteins elute at different ionic strengths in IEC column. WD4 elutes at much higher ionic strength compared to WD5-6 and this is a good basis for carrying

out metal transfer experiment that should be pursued to supplement the NMR titration results.

WD5-6 has two metal binding motifs, one in each domain. The discovery that this WD5-6 binds two equivalents of copper is consistent with the previous results which show that the 6 N-terminal MBDs of WDP is capable of binding up to 6 equivalents of Cu(I) (DiDonato et al., 1997).

The laser light scattering (LLS) experiment showed two peaks (Figure 14) which are clearly for WD5-6 in the monomeric and the dimeric state. WD5-6 is rich in cystein and is more likely to oxidize by forming inter-domain disulfide bonds and that explains the appearance of the dimer forms. Unlike the conventional SEC method, the molecular mass from LLS is independent of the elution volume. It therefore, can be used for sticky proteins which elute unusually late as a result of interaction with the column matrix.

Cu (I) did not cause aggregation because the apparent running mass for apo- and Cu (I) WD5-6 and are nearly the same (Table 7). Because WD5-6 is rich in Cys, it has the potential of forming intermolecular S-Cu-S links during titration of Cu (I) into the apo protein. The other likely causes of aggregation for cystein rich proteins like WD5-6 are intermolecular S-S links from oxidation of Cys residues by O_2. Aggregation status is critical for both structural and copper binding studies. WD5-6 was confirmed to be monomeric in reduced form by HRGC (Figure 13).

Preliminary data presented on chemical unfolding of WD5-6 forms a good basis for more unfolding and refolding experiments. Emission should be tested at more intermediary concentrations of guanidium chloride to enable calculation of unfolding energy of WD5-6. The results showed no peak shift in emission spectrum (Figure 19)

with increase in guanidium chloride concentration, but the decrease in fluorescence is not uniform with increase of denaturant concentration.

The use of heteronuclei, ^{15}N and ^{13}C, allows some new features in NMR which facilitate the structure determination, especially of larger proteins (more than 100 amino acids). However their natural abundance and gyromagnetic ratio are markedly lower than that of the proton (Table 9). Two strategies used to increase the low sensitivity of these nuclei are isotopic enrichment of these nuclei in proteins and enhancement of the signal to noise ratio by the use of inverse NMR experiment in which the magnetization is transferred from protons to the heteronucleus (HSQC). Other reasons for using ^{15}N and ^{13}C to label proteins are because they are not radioactive and therefore harmless and they have a spin of ½ and therefore can only have two quantum energy levels.

Isotope	Spin I	Natural abundance (%)	Gyromagnetic ratio(γ)	Relative sensitivity	Absolute sensitivity
^{1}H	½	99.98	26.7519	1.00	1.00
^{2}H	1	0.016	4.1066	$9.65*10^{-6}$	$1.45*10^{6}$
^{12}C	0	98.9	--	--	--
^{13}C	½	1.108	6.7283	$1.59*10^{-2}$	$1.76*10^{-4}$
^{14}N	1	99.63	1.9338	$1.01*10^{-3}$	$1.01*10^{-3}$
^{15}N	½	0.37	-2.712	$1.04*10^{-3}$	$1.04*10^{-3}$
^{16}O	0	98.9	--	--	--
^{17}O	5/2	0.037	-3.6279	$2.91*10^{-2}$	$1.08*10^{-5}$
^{31}P	½	100	10.841	$6.63*10^{-2}$	$6.63*10^{-2}$

Table 10. Most common isotopes encountered in biology and their relative abundance. Relative sensitivity is given at constant magnetic field and equal number of nuclei. Absolute sensitivity is the product of relative sensitivity multiplied by natural abundance.

The 1D NMR spectrum peaks for WD5-6 protein (Figure 20) showed good signal to noise ratio, which is indicative of a good condition for the NMR experiments. The

numerous chemical shift peaks seen for amide protons between 6.5- 9.5, for the alpha protons 3-5 and for aliphatic protons 0.5 to 3 is a clear indication that the sample was in a stable condition, optimal for NMR experiments. The 2D HSQC spectrum of WD5-6 (Figure 21) was consistent with the WD5-6 amino acid sequence and this is a key step in protein NMR. The 2D spectrum with ^{1}H and ^{15}N dimensions was used to determine whether the protein was well folded and is in optimal NMR experimental conditions, protein oligomeric status and quality control. WD5-6 is well folded because its HSQC spectrum of WD5-6 showed good dispersion of resonance. The sharp dispersed signals on HSQC spectrum is also a good indicator of optimal NMR experiment conditions and of the monomeric nature of WD5-6. Monomeric proteins show sharp signals on HSQC spectrum. HSQC is a good tool to probe whether the protein sample changes over a period of time and that for WD5-6 showed no peak shift over a period of six months.

The apoWD5-6 protein structure was shown to be organized in two subunits with ferrodoxin-like fold connected by a short linker (Figure 25). The fold of each subunit and their Cu binding sites structural properties are same to that found in the yeast homologue (Banci et al., 2001). The solution structure, hydrodynamic behavior, and relaxation parameters of WD5-6 reveal that this multidomain construct behaves as a unit in solution, with the metal binding domains facing away from each other, disallowing intramolecular Cu transfer between WD5 and WD6.

Copper binding produced spectral changes limited to the two Cu binding regions and did not affect its aggregation state as well as the overall structural properties. The observation that WD5-6 is able to accept Cu from another metal binding domain (WD4) and not from Atox1, as shown by NMR titration experiment, is consistent with earlier

evidence from yeast hybrid experiment which showed no interaction between the Atox1 and WD5-6 but showed a strong interaction between Atox1 and WD4 (van Dongen et al., 2004). No stable adduct was formed between WD5-6 and Cu(1)Atox1 but an adduct formed when WD4 was titrated with Cu(1)Atox1. These observations suggest that WD4 acquire cu from Atox1 and channel it through WD5-6 to the vesicular Cu pump.

The mechanism of adduct formation and Cu transfer between WD4 and WD5-6 may involve surface potential complimentarity between the two proteins. Atox1 has a similar positive surface region as Atx1 in the portion known to be involved in the interaction with Ccc2a, while WD5, 6 and Ccc2a have negative surface regions complimentary to those of Atox1 and Atx1. Atx1 is Cu chaperone that deliver Cu to Ccc2a protein in yeast (Rosenzweig *et al.*, 1999).

The other domain shown to interact with human copper chaperone, Atox1, is domain 2 (van Dongen et al., 2004; Walker et al., 2004) but it was shown that copper doesn't flow from this domain to the other domains (Walker et al., 2004). These results are not conclusive on the functional significance of copper binding to WD2. One suggestion was that copper binding to WD2 may trigger conformational changes in WDP leading to copper binding to the other domains. This would be consistent with the observation that a multi-domain construct of WD1-4 shows a stronger interaction with Atox1 than any one single domain.

The observation that Atox1 did not interact with WD5-6 raises the question as to what the effects of the 2 disease causing mutations in WD5-6 might be. This finding fails to support the earlier belief that the 2 mutations in the highly conserved residues interfere with interaction between the domains and the Atox1 and therefore Cu transfer between

N-WDP and Atox1. We have initiated studies aimed at characterizing the 2 mutations in WD5-6 with regards to Cu transfer between mutant WD5-6 and other WDP MBDs. We are also interested in understanding how the 2 disease causing mutations in the WD5-6 interfere with its function.

Conclusion

We have cloned and isolated WD5-6. We have shown that it binds 2 equivalents of copper, has a pI of 4.96 and α-helicity of 23%. We have shown by NMR spectroscopy that WD5-6 has a βαββαβ fold in each of the 2 domains and behaves as a unit in solution. We also showed by NMR titration that WD5-6 interacts with WD4 but not with Atox1.

REFERENCES

Anastassopoulou, I., Banci, L., Bertini, I., Cantini, F., Katsari, E., & Rosato, A. (2004). Solution structure of the apo and copper(i)-loaded human metallochaperone hah1. *Biochemistry, 43*(41), 13046-13053.

Arnesano, F., Banci, L., Bertini, I., Cantini, F., Ciofi-Baffoni, S., Huffman, D. L., et al. (2001). Characterization of the binding interface between the copper chaperone atx1 and the first cytosolic domain of ccc2 atpase. *J Biol Chem, 276*(44), 41365-41376.

Arnesano, F., Banci, L., Bertini, I., Ciofi-Baffoni, S., Molteni, E., Huffman, D. L., et al. (2002). Metallochaperones and metal-transporting atpases: A comparative analysis of sequences and structures. *Genome Res, 12*(2), 255-271.

Banci, L., Bertini, I., Ciofi-Baffoni, S., Huffman, D. L., & O'Halloran, T. V. (2001). Solution structure of the yeast copper transporter domain ccc2a in the apo and cu(i)-loaded states. *J Biol Chem, 276*(11), 8415-8426.

Banci, L., Bertini, I., Del Conte, R., D'Onofrio, M., & Rosato, A. (2004). Solution structure and backbone dynamics of the cu(i) and apo forms of the second metal-binding domain of the menkes protein atp7a. *Biochemistry, 43*(12), 3396-3403.

Brewer, G. J., & Yuzbasiyan-Gurkan, V. (1992). Wilson disease. *Medicine (Baltimore), 71*(3), 139-164.

Bull, P. C., & Cox, D. W. (1994). Wilson disease and menkes disease: New handles on heavy-metal transport. *Trends Genet, 10*(7), 246-252.

Carmichael, P. L., Hewer, A., Osborne, M. R., Strain, A. J., & Phillips, D. H. (1995). Detection of bulky DNA lesions in the liver of patients with wilson's disease and primary haemochromatosis. *Mutat Res, 326*(2), 235-243.

Christodoulou, J., Danks, D. M., Sarkar, B., Baerlocher, K. E., Casey, R., Horn, N., et al. (1998). Early treatment of menkes disease with parenteral copper-histidine: Long-term follow-up of four treated patients. *Am J Med Genet, 76*(2), 154-164.

Cox, D. W. (1999). Disorders of copper transport. *Br Med Bull, 55*(3), 544-555.

Culotta, V. C., Gitlin, JD. (2001). *Disorders of copper transport, the molecular and metabolic basis o inherited disease*. New York: McGraw-Hill.

Culotta, V. C., Lin, S. J., Schmidt, P., Klomp, L. W., Casareno, R. L., & Gitlin, J. (1999). Intracellular pathways of copper trafficking in yeast and humans. *Adv Exp Med Biol, 448*, 247-254.

Danks, D. M. (1980). Copper deficiency in humans. *Ciba Found Symp, 79*, 209-225.

Danks, D. M. (1995). *Disorders of copper transport*. New York: McGraw Hill.

DiDonato, M., Hsu, H. F., Narindrasorasak, S., Que, L., Jr., & Sarkar, B. (2000). Copper-induced conformational changes in the n-terminal domain of the wilson disease copper-transporting atpase. *Biochemistry, 39*(7), 1890-1896.

DiDonato, M., Narindrasorasak, S., Forbes, J. R., Cox, D. W., & Sarkar, B. (1997). Expression, purification, and metal binding properties of the n-terminal domain from the wilson disease putative copper-transporting atpase (atp7b). *J Biol Chem, 272*(52), 33279-33282.

DiDonato, M., Zhang, J., Que, L., Jr., & Sarkar, B. (2002). Zinc binding to the nh2-terminal domain of the wilson disease copper-transporting atpase: Implications

for in vivo metal ion-mediated regulation of atpase activity. *J Biol Chem, 277*(16), 13409-13414.

DiGuiseppi, J., & Fridovich, I. (1984). The toxicology of molecular oxygen. *Crit Rev Toxicol, 12*(4), 315-342.

Elam, J. S., Thomas, S. T., Holloway, S. P., Taylor, A. B., & Hart, P. J. (2002). Copper chaperones. *Adv Protein Chem, 60*, 151-219.

Fatemi, N., & Sarkar, B. (2002). Molecular mechanism of copper transport in wilson disease. *Environ Health Perspect, 110 Suppl 5*, 695-698.

Forbes, J. R., Hsi, G., & Cox, D. W. (1999). Role of the copper-binding domain in the copper transport function of atp7b, the p-type atpase defective in wilson disease. *J Biol Chem, 274*(18), 12408-12413.

Frommer, D. J. (1974). Defective biliary excretion of copper in wilson's disease. *Gut, 15*(2), 125-129.

Frydman, M., Bonne-Tamir, B., Farrer, L. A., Conneally, P. M., Magazanik, A., Ashbel, S., et al. (1985). Assignment of the gene for wilson disease to chromosome 13: Linkage to the esterase d locus. *Proc Natl Acad Sci U S A, 82*(6), 1819-1821.

Gitlin, J. D. (2003). Wilson disease. *Gastroenterology, 125*(6), 1868-1877.

Gitschier, J., Moffat, B., Reilly, D., Wood, W. I., & Fairbrother, W. J. (1998). Solution structure of the fourth metal-binding domain from the menkes copper-transporting atpase. *Nat Struct Biol, 5*(1), 47-54.

Gollan, J. L., & Gollan, T. J. (1998). Wilson disease in 1998: Genetic, diagnostic and therapeutic aspects. *J Hepatol, 28 Suppl 1*, 28-36.

Gross, C., Kelleher, M., Iyer, V. R., Brown, P. O., & Winge, D. R. (2000). Identification of the copper regulon in saccharomyces cerevisiae by DNA microarrays. *J Biol Chem, 275*(41), 32310-32316.

Gu, M., Cooper, J. M., Butler, P., Walker, A. P., Mistry, P. K., Dooley, J. S., et al. (2000). Oxidative-phosphorylation defects in liver of patients with wilson's disease. *Lancet, 356*(9228), 469-474.

Hamza, I., Faisst, A., Prohaska, J., Chen, J., Gruss, P., & Gitlin, J. D. (2001). The metallochaperone atox1 plays a critical role in perinatal copper homeostasis. *Proc Natl Acad Sci U S A, 98*(12), 6848-6852.

Hamza, I., Schaefer, M., Klomp, L. W., & Gitlin, J. D. (1999). Interaction of the copper chaperone hah1 with the wilson disease protein is essential for copper homeostasis. *Proc Natl Acad Sci U S A, 96*(23), 13363-13368.

Huang, X., Cuajungco, M. P., Atwood, C. S., Hartshorn, M. A., Tyndall, J. D., Hanson, G. R., et al. (1999). Cu(ii) potentiation of alzheimer abeta neurotoxicity. Correlation with cell-free hydrogen peroxide production and metal reduction. *J Biol Chem, 274*(52), 37111-37116.

Huffman, D. L., & O'Halloran, T. V. (2001). Function, structure, and mechanism of intracellular copper trafficking proteins. *Annu Rev Biochem, 70*, 677-701.

Hung, I. H., Suzuki, M., Yamaguchi, Y., Yuan, D. S., Klausner, R. D., & Gitlin, J. D. (1997). Biochemical characterization of the wilson disease protein and functional expression in the yeast saccharomyces cerevisiae. *J Biol Chem, 272*(34), 21461-21466.

Huster, D., & Lutsenko, S. (2003). The distinct roles of the n-terminal copper-binding sites in regulation of catalytic activity of the wilson's disease protein. *J Biol Chem, 278*(34), 32212-32218.

Iida, M., Terada, K., Sambongi, Y., Wakabayashi, T., Miura, N., Koyama, K., et al. (1998). Analysis of functional domains of wilson disease protein (atp7b) in saccharomyces cerevisiae. *FEBS Lett, 428*(3), 281-285.

Jensen, P. Y., Bonander, N., Horn, N., Tumer, Z., & Farver, O. (1999). Expression, purification and copper-binding studies of the first metal-binding domain of menkes protein. *Eur J Biochem, 264*(3), 890-896.

Kay, L. E., Torchia, D. A., & Bax, A. (1989). Backbone dynamics of proteins as studied by 15n inverse detected heteronuclear nmr spectroscopy: Application to staphylococcal nuclease. *Biochemistry, 28*(23), 8972-8979.

Krawczak, M., & Cooper, D. N. (1997). The human gene mutation database. *Trends Genet, 13*(3), 121-122.

Larin, D., Mekios, C., Das, K., Ross, B., Yang, A. S., & Gilliam, T. C. (1999). Characterization of the interaction between the wilson and menkes disease proteins and the cytoplasmic copper chaperone, hah1p. *J Biol Chem, 274*(40), 28497-28504.

Lavelle, F., Michelson, A. M., & Dimitrijevic, L. (1973). Biological protection by superoxide dismutase. *Biochem Biophys Res Commun, 55*(2), 350-357.

Lee, J., Pena, M. M., Nose, Y., & Thiele, D. J. (2002). Biochemical characterization of the human copper transporter ctr1. *J Biol Chem, 277*(6), 4380-4387.

Lee, J., Prohaska, J. R., & Thiele, D. J. (2001). Essential role for mammalian copper transporter ctr1 in copper homeostasis and embryonic development. *Proc Natl Acad Sci U S A, 98*(12), 6842-6847.

Linder, M. C. (1991). *Biochemistry of copper*. New York: Plenum Press.

Lockhart, P. J., & Mercer, J. F. (2000). Identification of the copper chaperone sah in ovis aries: Expression analysis and in vitro interaction of sah with atp7b. *Biochim Biophys Acta, 1490*(1-2), 11-20.

Loudianos, G., Dessi, V., Angius, A., Lovicu, M., Loi, A., Deiana, M., et al. (1996). Wilson disease mutations associated with uncommon haplotypes in mediterranean patients. *Hum Genet, 98*(6), 640-642.

Lutsenko, S., Efremov, R. G., Tsivkovskii, R., & Walker, J. M. (2002). Human copper-transporting atpase atp7b (the wilson's disease protein): Biochemical properties and regulation. *J Bioenerg Biomembr, 34*(5), 351-362.

Mitra, B., & Sharma, R. (2001). The cysteine-rich amino-terminal domain of znta, a pb(ii)/zn(ii)/cd(ii)-translocating atpase from escherichia coli, is not essential for its function. *Biochemistry, 40*(25), 7694-7699.

Nair, J., Carmichael, P. L., Fernando, R. C., Phillips, D. H., Strain, A. J., & Bartsch, H. (1998). Lipid peroxidation-induced etheno-DNA adducts in the liver of patients with the genetic metal storage disorders wilson's disease and primary hemochromatosis. *Cancer Epidemiol Biomarkers Prev, 7*(5), 435-440.

O'Halloran, T. V., & Culotta, V. C. (2000). Metallochaperones, an intracellular shuttle service for metal ions. *J Biol Chem, 275*(33), 25057-25060.

Odermatt, A., Suter, H., Krapf, R., & Solioz, M. (1993). Primary structure of two p-type atpases involved in copper homeostasis in enterococcus hirae. *J Biol Chem, 268*(17), 12775-12779.

Paschen, W., & Weser, U. (1973). Letter: Singlet oxygen decontaminating activity of erythrocuprein (superoxide dismutase). *Biochim Biophys Acta, 327*(1), 217-222.

Payne, A. S., & Gitlin, J. D. (1998). Functional expression of the menkes disease protein reveals common biochemical mechanisms among the copper-transporting p-type atpases. *J Biol Chem, 273*(6), 3765-3770.

Pena, M. M., Lee, J., & Thiele, D. J. (1999). A delicate balance: Homeostatic control of copper uptake and distribution. *J Nutr, 129*(7), 1251-1260.

Peng, J. W., & Wagner, G. (1992). Mapping of the spectral densities of n-h bond motions in eglin c using heteronuclear relaxation experiments. *Biochemistry, 31*(36), 8571-8586.

Pervushin, K., Riek, R., Wider, G., & Wuthrich, K. (1997). Attenuated t2 relaxation by mutual cancellation of dipole-dipole coupling and chemical shift anisotropy indicates an avenue to nmr structures of very large biological macromolecules in solution. *Proc Natl Acad Sci U S A, 94*(23), 12366-12371.

Prohaska, J. R., & Gybina, A. A. (2004). Intracellular copper transport in mammals. *J Nutr, 134*(5), 1003-1006.

Pufahl, R. A., Singer, C. P., Peariso, K. L., Lin, S. J., Schmidt, P. J., Fahrni, C. J., et al. (1997). Metal ion chaperone function of the soluble cu(i) receptor atx1. *Science, 278*(5339), 853-856.

Puig, S., Lee, J., Lau, M., & Thiele, D. J. (2002). Biochemical and genetic analyses of yeast and human high affinity copper transporters suggest a conserved mechanism for copper uptake. *J Biol Chem, 277*(29), 26021-26030.

Rae, T. D., Schmidt, P. J., Pufahl, R. A., Culotta, V. C., & O'Halloran, T. V. (1999). Undetectable intracellular free copper: The requirement of a copper chaperone for superoxide dismutase. *Science, 284*(5415), 805-808.

Ralle, M., Lutsenko, S., & Blackburn, N. J. (2003). X-ray absorption spectroscopy of the copper chaperone hah1 reveals a linear two-coordinate cu(i) center capable of adduct formation with exogenous thiols and phosphines. *J Biol Chem, 278*(25), 23163-23170.

Rosenzweig, A. C., Huffman, D. L., Hou, M. Y., Wernimont, A. K., Pufahl, R. A., & O'Halloran, T. V. (1999). Crystal structure of the atx1 metallochaperone protein at 1.02 a resolution. *Structure Fold Des, 7*(6), 605-617.

Schaefer, M., & Gitlin, J. D. (1999). Genetic disorders of membrane transport. Iv. Wilson's disease and menkes disease. *Am J Physiol, 276*(2 Pt 1), G311-314.

Scheinberg, I. H., & Gitlin, D. (1952). Deficiency of ceruloplasmin in patients with hepatolenticular degeneration (wilson's disease). *Science, 116*(3018), 484-485.

Solioz, M., & Vulpe, C. (1996). Cpx-type atpases: A class of p-type atpases that pump heavy metals. *Trends Biochem Sci, 21*(7), 237-241.

Sternlieb, I. (1984). Wilson's disease: Indications for liver transplants. *Hepatology, 4*(1 Suppl), 15S-17S.

Strausak, D., La Fontaine, S., Hill, J., Firth, S. D., Lockhart, P. J., & Mercer, J. F. (1999). The role of gmxcxxc metal binding sites in the copper-induced redistribution of the menkes protein. *J Biol Chem, 274*(16), 11170-11177.

Tao, T. Y., & Gitlin, J. D. (2003). Hepatic copper metabolism: Insights from genetic disease. *Hepatology, 37*(6), 1241-1247.

Tao, T. Y., Liu, F., Klomp, L., Wijmenga, C., & Gitlin, J. D. (2003). The copper toxicosis gene product murr1 directly interacts with the wilson disease protein. *J Biol Chem, 278*(43), 41593-41596.

Tonnesen, T., Petterson, A., Kruse, T. A., Gerdes, A. M., & Horn, N. (1992). Multipoint linkage analysis in menkes disease. *Am J Hum Genet, 50*(5), 1012-1017.

Tsay, M. J., Fatemi, N., Narindrasorasak, S., Forbes, J. R., & Sarkar, B. (2004). Identification of the "missing domain" of the rat copper-transporting atpase, atp7b: Insight into the structural and metal binding characteristics of its n-terminal copper-binding domain. *Biochim Biophys Acta, 1688*(1), 78-85.

Tsukihara, T., Aoyama, H., Yamashita, E., Tomizaki, T., Yamaguchi, H., Shinzawa-Itoh, K., et al. (1995). Structures of metal sites of oxidized bovine heart cytochrome c oxidase at 2.8 a. *Science, 269*(5227), 1069-1074.

van Dongen, E. M., Klomp, L. W., & Merkx, M. (2004). Copper-dependent protein-protein interactions studied by yeast two-hybrid analysis. *Biochem Biophys Res Commun, 323*(3), 789-795.

Vanderwerf, S. M., Cooper, M. J., Stetsenko, I. V., & Lutsenko, S. (2001). Copper specifically regulates intracellular phosphorylation of the wilson's disease protein, a human copper-transporting atpase. *J Biol Chem, 276*(39), 36289-36294.

Viles, J. H., Cohen, F. E., Prusiner, S. B., Goodin, D. B., Wright, P. E., & Dyson, H. J. (1999). Copper binding to the prion protein: Structural implications of four identical cooperative binding sites. *Proc Natl Acad Sci U S A, 96*(5), 2042-2047.

Voskoboinik, I., Mar, J., Strausak, D., & Camakaris, J. (2001). The regulation of catalytic activity of the menkes copper-translocating p-type atpase. Role of high affinity copper-binding sites. *J Biol Chem, 276*(30), 28620-28627.

Voskoboinik, I., Strausak, D., Greenough, M., Brooks, H., Petris, M., Smith, S., et al. (1999). Functional analysis of the n-terminal cxxc metal-binding motifs in the human menkes copper-transporting p-type atpase expressed in cultured mammalian cells. *J Biol Chem, 274*(31), 22008-22012.

Vulpe, C., Levinson, B., Whitney, S., Packman, S., & Gitschier, J. (1993). Isolation of a candidate gene for menkes disease and evidence that it encodes a copper-transporting atpase. *Nat Genet, 3*(1), 7-13.

Walker, J. M., Huster, D., Ralle, M., Morgan, C. T., Blackburn, N. J., & Lutsenko, S. (2004). The n-terminal metal-binding site 2 of the wilson's disease protein plays a key role in the transfer of copper from atox1. *J Biol Chem, 279*(15), 15376-15384.

Walker, J. M., Tsivkovskii, R., & Lutsenko, S. (2002). Metallochaperone atox1 transfers copper to the nh2-terminal domain of the wilson's disease protein and regulates its catalytic activity. *J Biol Chem, 277*(31), 27953-27959.

Wernimont, A. K., Huffman, D. L., Lamb, A. L., O'Halloran, T. V., & Rosenzweig, A. C. (2000). Structural basis for copper transfer by the metallochaperone for the menkes/wilson disease proteins. *Nat Struct Biol, 7*(9), 766-771.

Wernimont, A. K., Yatsunyk, L. A., & Rosenzweig, A. C. (2004). Binding of copper(i) by the wilson disease protein and its copper chaperone. *J Biol Chem, 279*(13), 12269-12276.

Wilson, S. (1912). Progressive lenticular degenaration: A familial nervous disease associated with cirrhosis of the liver. *Brain, 34*, 295-508.

Yuan, D. S., Stearman, R., Dancis, A., Dunn, T., Beeler, T., & Klausner, R. D. (1995). The menkes/wilson disease gene homologue in yeast provides copper to a ceruloplasmin-like oxidase required for iron uptake. *Proc Natl Acad Sci U S A, 92*(7), 2632-2636.